Basin Research (1997) **9,** 1–26

Sedimentary sequences, seismofacies and evolution of depositional systems of the Oligo/Miocene Lower Freshwater Molasse Group, Switzerland

F. Schlunegger,* A. Matter,* D. W. Burbank,† W. Leu,‡ M. Mange§ and J. Màtyàs*

**Geologisches Institut, Universität Bern, Baltzerstrasse 1, CH-3012 Bern, Switzerland*
†Department of Earth Sciences, University of Southern California, Los Angeles, CA 90089–0740, USA
‡Geoform AG, 8401 Winterthur, Switzerland
§University of Oxford, Department of Earth Sciences, Parks Road, Oxford OS1 3PR, UK

ABSTRACT

Magnetostratigraphic chronologies, together with sedimentological, petrological, seismic and borehole data derived from the Oligo/Miocene Lower Freshwater Molasse Group of the North Alpine foreland basin enable a detailed reconstruction of alluvial architecture in relation to Alpine orogenic events. Six depositional systems are recorded in the Lower Freshwater Molasse Group. The bajada depositional system comprises 200–400-m-thick successions of ribbon channel conglomerates and overbank fines including mud- and debris-flows which were derived from the Alpine border chain. The alluvial megafan depositional system is made up of massive pebble-to-cobble conglomerates up to 3 km thick which reveal a fan-shaped geometry. This depositional environment grades downcurrent into the conglomerate channel belt depositional system, which comprises an $\approx$2-km-thick alternation of channel conglomerates and overbank fines. The sandstone channel belt depositional system is bordered by the 100–400-m-thick overbank fines assigned to the floodplain depositional system. At the feather edge of the basin, 50–400-m-thick lacustrine sediments in both clastic and carbonate facies represent the lacustrine depositional system.

The spatial and temporal arrangement of these depositional systems was controlled by the geometrical evolution of the Molasse Basin. During periods of enhanced sediment supply and during phases of stable sliding of the entire wedge, $>$2000-m-thick coarsening-and thickening-upward megasequences comprising the conglomerate channel belt, alluvial megafan and bajada depositional systems were deposited in a narrow wedge-shaped basin. In the distal reaches of the basin, however, no sedimentary trend developed, and the basin fill comprises a $<$500-m-thick series of sandstone meander belt, floodplain and lacustrine depositional systems. During phases of accretion at the toe of the wedge, the basin widened, and prograding systems of multistorey channel sandstones extended from the thrust front to the distal reaches of the basin.

The rearrangement of the depositional systems as a function of changing orogenic conditions created discordances, which are expressed seismically by onlap and erosion of beds delimiting sedimentary sequences. Whereas stable sliding of the wedge succeeded by accretion at the toe of the wedge is recorded in the proximal Lower Freshwater Molasse by a coarsening- and thickening-upward megasequence followed by erosion, the opposite trend developed in the distal reaches of the Molasse. Here, fine-grained sandstones and mudstones were deposited during periods of stable sliding, whereas phases of accretion caused a coarsening- and thickening-up megasequence to form.

INTRODUCTION

Foreland basins form as a mechanical response to crustal thickening in the adjacent orogenic wedge (Beaumont, 1981; Jordan, 1981). Because of the sensitivity of foreland basins to tectonic events in the neighbouring fold and thrust belt, the stratigraphies of these basins have been used to assess the loading history of the hinterland (Burbank *et al.,* 1986; Anadón *et al.,* 1986; Jordan *et al.,* 1988; Burbank *et al.,* 1992). Tectonic processes that control the stratigraphy and geometry of foreland basins include stable sliding of the entire wedge, accretion at the toe of the wedge as well as crustal thickening/thinning in the rear of the wedge (Sinclair *et al.,* 1991). Erosional denudation is a further parameter that significantly affects the evolution of foreland basins. According to Flemings & Jordan (1989, 1990), erosion and transport of sediment into the foreland basin decreases the orogenic load and increases the sediment load of the basin. As a result, the foreland basin widens, and facies boundaries prograde. Hence, it is the complex interaction between the sediment supply and the rate at which accommodation space is generated by tectonic loads that controls the geometry and the large-scale architecture of foreland basins (Sinclair & Allen, 1992).

A successful reconstruction of the relationships between the evolution of orogens and their foreland basins requires (i) profound knowledge of the structural evolution of the hinterland determined independently from cooling ages and sediment-accumulation rate patterns, (ii) cooling ages to assess the sediment flux and (iii) a high-resolution reconstruction of the architecture of the adjacent foreland basin. The Oligo–Miocene Alps/Molasse Basin system meet most of these requirements. Because of the extensive structural, chronological and stratigraphical data available for this system (Diem, 1986; Pfiffner, 1986; Keller, 1989; Hunziker *et al.,* 1992; Schlunegger, 1995; Schmid *et al.,* 1996), it has been a classical area to document the influence of orogenic thickening and erosional denudation in the Alps on the large-scale stratigraphic evolution of the Molasse Basin (Homewood *et al.,* 1986; Pfiffner, 1986; Sinclair *et al.,* 1991; Sinclair & Allen, 1992; Burbank *et al.,* 1992; Schlunegger *et al.,* 1993). These studies mainly concentrated on the proximal part of the Molasse Basin because of large variations in lithofacies and accumulation rates. However, until recently when seismic data became public and detailed temporal control using magnetostratigraphy was established (Schlunegger *et al.,* 1996a), such attempts to link basin fill history with Alpine thrust wedge evolution remained rather speculative. Using high-resolution magnetostratigraphy, sedimentary petrography and facies analysis Schlunegger *et al.* (1996b) described the temporal relationships between the evolution of the proximal Swiss Molasse Basin and Alpine tectonic events.

In this paper, we reconstruct the sedimentary sequences and the depositional systems of the Lower Freshwater Molasse in a section across the central Swiss Molasse Basin from the thrust front to its feather-edge. The reconstruction is based on a combination of detailed facies analysis on outcrops, wells and seismic sections. Both the evolution of the depositional systems in relation to crustal thickening and erosional denudation in the orogen and the changes of the drainage systems through space and time are discussed in the detailed temporal framework provided by magnetostratigraphy.

GEOLOGICAL SETTING

The present-day Alps are the result of the Oligo/Miocene continent–continent collision between the Adriatic promontory of Africa and the European plate, which resulted in a total of 120 km of post-Eocene shortening (Schmid *et al.,* 1996). In the north, the Alpine edifice consists of the Helvetic zone, which is subdivided into a lower Infrahelvetic complex (Aar massif and its autochthonous–parautochthonous cover) and an upper Helvetic (sensu stricto) complex (Helvetic thrust nappes), separated by the Glarus thrust (Fig. 1A, B). The Helvetic zone, in turn, is overlain by a piggyback stack of Penninic and Austroalpine sedimentary and crystalline nappes. The southern Alps comprise a thin-skinned and a thick-skinned stack of Adriatic crust (Schönborn, 1992). They are separated from the northern Alps by the E–W-striking Insubric Line, which partly accommodated the indentation of the Adriatic promontory by steep S-directed synmagmatic reverse faulting and right lateral strike-slip movements (Pfiffner, 1992; Schmid *et al.,* 1996).

The sedimentological development of the North Alpine foreland basin can be described in terms of an early deep-water stage and a later shallow-water/continental stage which has been referred to as 'Flysch' and 'Molasse' in the classic Alpine literature (see discussions in Sinclair *et al.,* 1991; Sinclair & Allen, 1992). The 'Molasse' has been traditionally divided into four lithostratigraphic units, for which the conventional German abbreviations are used in this paper (Matter *et al.,* 1980; Keller, 1989; Fig. 2): Lower Marine Molasse (UMM), Lower Freshwater Molasse (USM), Upper Marine Molasse (OMM) and Upper Freshwater Molasse (OSM). They form two shallowing-upward megasequences . The first megasequence comprises the Rupelian UMM, which is followed by the Chattian and Aquitanian fluvial clastics of the USM. The second megasequence, starting with the Burdigalian transgression, consists of shallow-marine sandstones (OMM), which interfinger with major fan deltas adjacent to the thrust front (Berli, 1985; Keller, 1989; Hurni, 1991; Schlunegger *et al.,* 1993). It ends with Serravalian fluvial clastics of the OSM.

The studied section runs from the thrusted Subalpine Molasse of central Switzerland across the mainly flat-lying Plateau Molasse (Fig. 2). The Lower Freshwater Molasse Group has a total preserved thickness of *c*. 4 km at the Alpine front and thins to 70 m near the feather-edge of the basin (Baumberger, 1927; Homewood *et al.,*

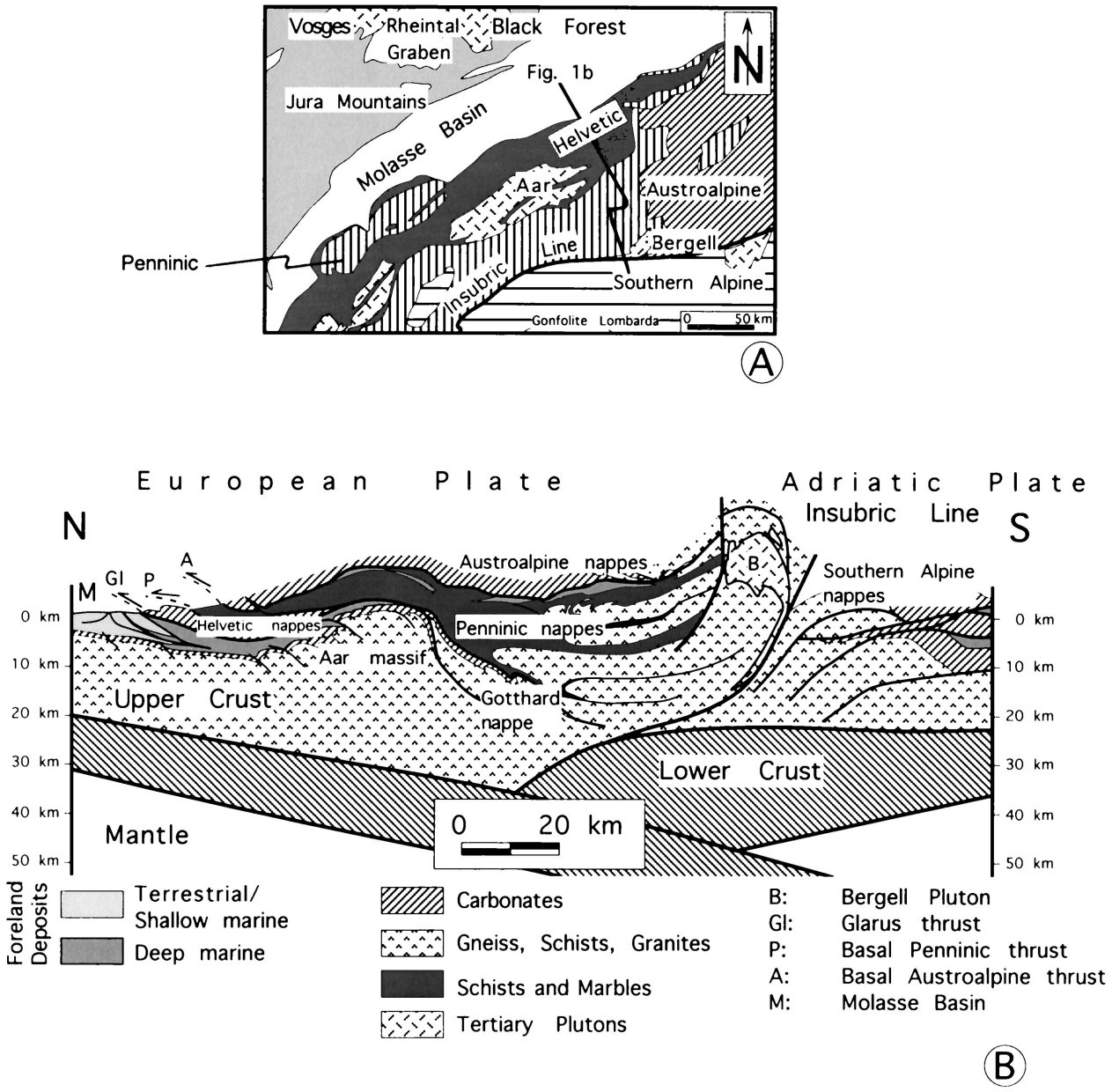

Fig. 1. (A) Geological map of the Oligo-Miocene Swiss Molasse Basin and the adjacent Alpine orogen. The major tectonic units are labelled. (B) Synthetic cross-section through the present-day Alpine hinterland. (Modified after Schmid *et al.*, 1996.)

1986). In the proximal part it consists mainly of alluvial megafan conglomerates which pass downcurrent into channel conglomerates and channel sandstones bordered by alluvial plain mudstones and lacustrine carbonates (Büchi & Schlanke, 1977; Platt & Keller, 1992).

The proximal USM exposed in the Subalpine thrust belt consists of two coarsening- and thickening-upward sequences going from mudstones to conglomerates. They were deposited between 30–25.5 and 24–21.5 Ma, respectively (Schlunegger *et al.*, 1996b). Cross-cutting relationships between calibrated metamorphic fabrics in the Helvetic zone (Milnes & Pfiffner, 1977, 1980) and the presence of reworked Oligocene conglomerates in the second sequence (Schlunegger *et al.*, 1996b) indicate that the construction of the two sequences coincides with thrusting along the Glarus thrust (30–25 Ma, Fig. 1) and uplift of the Subalpine Molasse (24–21.5 Ma, Schlunegger *et al.*, 1996b). Furthermore, petrographic data reveal that the USM was deposited by three major dispersal systems (Rigi, Höhronen, Napf) originating in the Penninic and Austroalpine nappes (Fig. 1) (Kleiber, 1937; Speck, 1937; Füchtbauer, 1959, 1964; Matter, 1964; Gasser, 1966, 1968; Müller, 1971; Stürm, 1973; Schlanke, 1974; Matter *et al.*, 1988a, b).

In contrast to the proximal USM, the distal strata are poorly exposed because of a dense vegetational cover as well as overlying Burdigalian to Quaternary deposits. Nevertheless, quarry exposures and boreholes allowed Platt & Keller (1992) a detailed facies analysis of the upper (Aquitanian) part of the USM. These authors

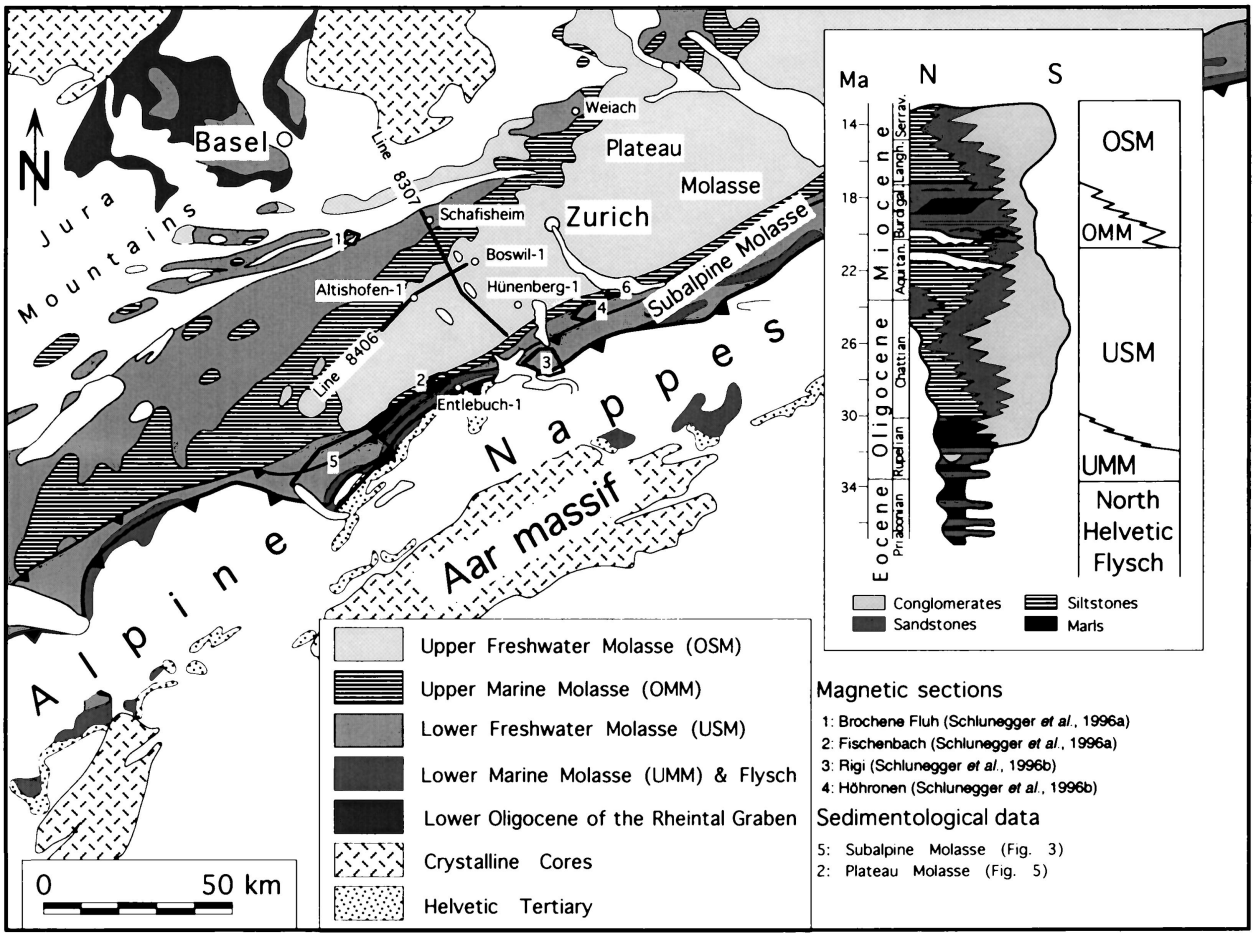

Fig. 2. Geological map of the Oligo-Miocene Swiss Molasse Basin and the adjacent Alpine orogen with a general stratigraphy of the foreland basin and the location of the study area, the seismic lines, the boreholes and the exposed sections (modified after Schlunegger *et al.,* 1996a). NHF: North Helvetic Flysch, UMM: Lower Marine Molasse, USM: Lower Freshwater Molasse, OSM: Upper Freshwater Molasse.

revealed that the variety of lithofacies in the distal USM can be summarized into five distinct sedimentological units referred to as intermediate-scale architectural elements (Platt & Keller, 1992): meander belt sandstones, crevasse channel and crevasse splay sandstones, levee sandstones and siltstones, overbank mudstones and palaeosols as well as lacustrine siltstones. Until now, no detailed sedimentological facies analysis nor a basin-wide facies reconstruction of the entire USM has been attempted.

METHODS

In order to unravel the evolution of the depositional systems in the Lower Freshwater Molasse Group, a number of techniques were employed, including sedimentological and petrographic facies analysis, magnetostratigraphy of outcrop sections and boreholes, and seismostratigraphy. Eight sections with a total thickness of $\approx$7000 m were logged in detail for lithofacies and sedimentary structures (for detailed sedimentological logs refer to Schlunegger, 1995). These field studies provided the framework for architectural facies analysis in terms of Miall (1985, 1988) and Platt & Keller (1992). In addition, the three-dimensional arrangement of the architectural elements was studied on large exposures. The architecture of the wells Schafisheim, Hünenberg-1, Boswil-1 and Altishofen-1 (Fig. 2) is reconstructed based on the sedimentological interpretation of mudlog data, available cores and gamma ray and sonic logs, using the methodology described in detail by Blaser *et al.* (1994).

The petrofacies data taken from Matter (1964), Gasser (1966), Stürm (1973), Schlanke (1974) and Schlunegger *et al.* (1996b) comprise conglomerate clast counts and determination of heavy mineral composition of sandstones. In addition, 33 heavy mineral analyses were carried out on cuttings from the Boswil-1 and Schafisheim wells using the method described by Schlunegger *et al.* (1993). A seismic line across the Plateau Molasse (line 8307) was analysed using seismostratigraphic techniques (Mitchum, 1977; Mitchum & Vail, 1977; Beer *et al.,* 1990; Cross *et al.,* 1993; Vakarcs *et al.,* 1994). First, discordances were identified using regional onlap and truncation of reflections in order to delimit sedimentary sequences. Second, seismic facies were defined based on length of reflections, amplitudes and frequencies. They

were mapped in the seismic section and interpreted in terms of depositional systems. Calibration of the seismic facies was achieved using the reconstructed sedimentological data of the neighbouring boreholes. Time–depth conversion was calculated based on the velocities determined in these boreholes. The magnetostratigraphic calibration of the sections in the Subalpine Molasse (Fig. 2) is taken from Schlunegger *et al.* (1996a, b). The chronological framework of the Plateau Molasse was completed using high-resolution magnetostratigraphy established on two boreholes (Weiach, Altishofen, Fig. 2) and on an outcrop section located at the feather-edge of the basin (Brochene Fluh section, Fig. 2; Schlunegger *et al.,* 1996a). The time-calibrated horizons of the Altishofen section were then correlated with the analysed cross-section using an E–W seismic line (line 8406, Fig. 2).

For the magnetostratigraphic analysis of the Weiach and Altishofen sections, brown to yellow laminated or massive mudstones were preferentially sampled. In addition, laminated siltstones and fine-grained sandstones were collected if no other suitable lithologies were available. Samples were taken every 5 m, depending on availability of fine-grained material. Four to five specimens were collected for each site. Detailed demagnetization analysis of specimens from different portions of the basin and different depositional systems revealed that characteristic remnant magnetizations are found in the 250–350 °C temperature window (Burbank *et al.,* 1992; Schlunegger *et al.,* 1996a). Subsequently, all specimens were demagnetized through temperatures of 250, 300 and 350 °C to reveal their characteristic remanence. Measured declinations of the samples were strongly offset because of horizontal rotation of the core during drilling. However, the same orientation of specimens from the same site allowed comparison of measured inclination and rotated declination vectors using Fisher (1953) statistics. Sites were classified as class I if $K \geq 10$ for three specimens. They were classified as class II if $K < 10$ for three specimens and $K \geq 10$ for two specimens.

RESULTS

Depositional systems

The concept of sedimentary architecture applied to fluvial deposits has proven very helpful for reconstructing the physical processes of ancient rivers and the resulting stratigraphy (Bromley, 1991; Lang & Fielding, 1991; Miall, 1991; Nadon, 1994). It has been used to break down the depositional sequence into a hierarchy of architectural elements, representing different orders of magnitude of time (Keller, 1993). The architectural elements defined by Platt & Keller (1992) in the USM comprise groups 6–7 (single to composite macroforms) of Miall (1991) which are interpreted to record processes between 10^2 and 10^4 years. Fluvial processes of these time spans are controlled by intrinsic mechanisms, whereas occurrence of architectural elements of longer duration, such as alluvial megafans or channel belts, are responses to extrinsic factors (e.g. Burbank & Beck, 1991; Miall, 1991). These depositional systems, which represent architectural elements of a gigascopic scale (Keller, 1993), will be presented in the following section.

Alluvial Megafan depositional system

This depositional system consists of predominantly pebble to cobble conglomerates with maximum clasts measuring between 20 and 50 cm in diameter (Schlunegger *et al.,* 1993). Its thickness may exceed 3 km in the coarsest grained part, and its lateral extent varies from 3 to 15 km (Figs 3 and 4). Typically it shows a fan-shaped geometry in map-view (Fig. 3). This system is composed of individual, lens-shaped 1–2-m-thick and several-metre-wide clast-supported, well-rounded and moderately sorted massive conglomerate beds. They form composite units up to 10 m thick and tens to hundreds of metres wide separated by decimetre-thick red silty layers. Occasionally matrix-supported conglomerates, as well as horizontally bedded well-sorted conglomerates with imbricated clasts, also occur.

Interpretation

The coarseness of the conglomerates as well the fan geometry (Fig. 3) suggests the presence of alluvial megafans (Sinha & Friend, 1994). The composite units with internal erosional surfaces separating the lens-shaped conglomerate beds are interpreted as lobes, consisting of individual gravel bars (Rust, 1978; Miall, 1978, 1985). Switching of drainage axes causes de-activation of the lobe and fine-grained material can be deposited during waning floods. Note that in this paper, the term 'megafan' as used by Gohain & Parkash (1990), Parkash & Kumar (1991) and Singh *et al.* (1993) is favoured to avoid confusion with the smaller, higher gradient, features generally called 'fans' by sedimentary geologists (Blair & McPherson, 1994a, b).

Bajada depositional system

Yellowish mottled mudstones with isolated conglomerate and sandstone bodies form 200–400-m-thick successions (Fig. 4). The mudstones, measuring up to 50 m thick, are either massive with scattered pebbles, or decimetre-bedded and graded. The moderately sorted cobble to boulder conglomerates are less than 3 m thick, deeply incised and pinch out laterally within a few metres. Vertical stacking of 2–5 beds leads to 12–15-m-thick conglomerate bodies of limited lateral extent. The clast-supported conglomerates may be either unstratified or cross-bedded. Moreover, thin (20–50 cm) and only 2–3-m-wide pebble-conglomerate lenses with weakly erosional bases and inverse grading occur scattered in the

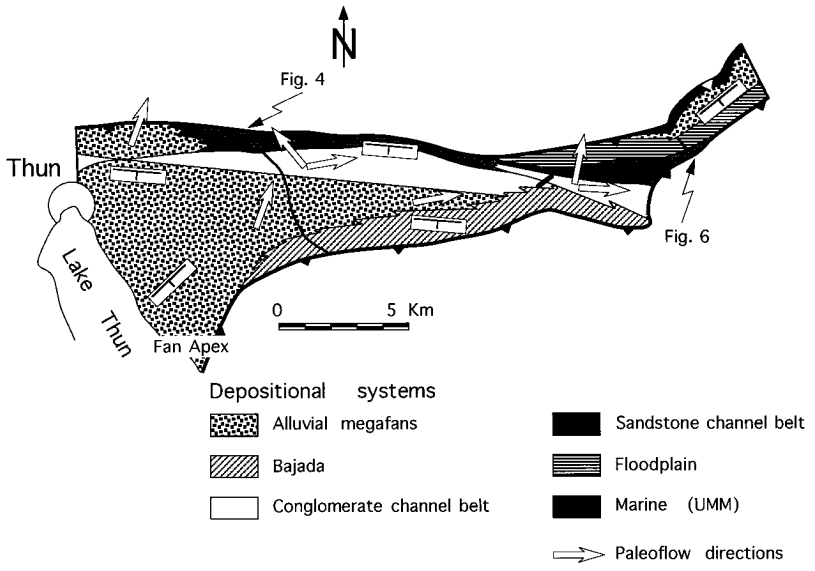

Fig. 3. Sedimentological map of the proximal basin border (see Fig. 2 for location) indicating the geometries of the depositional systems and the location of the measured sections.

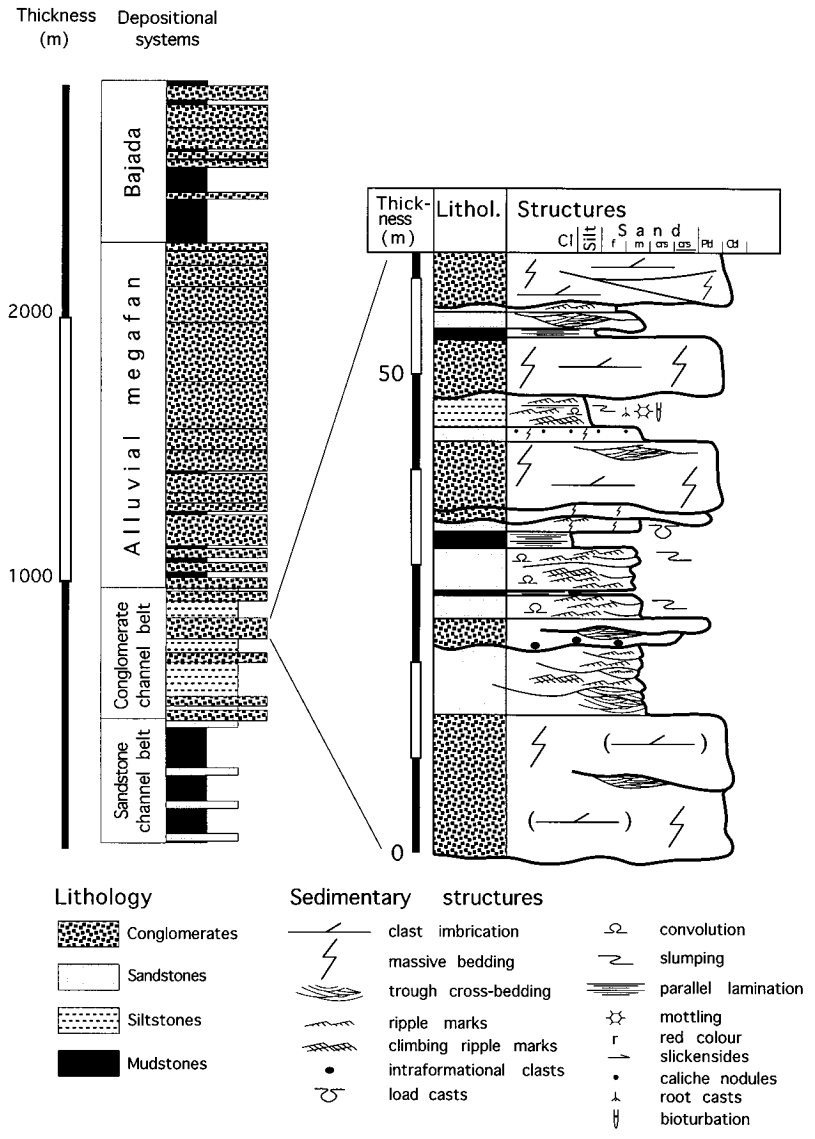

Fig. 4. Stratigraphy of the proximal USM with detailed sedimentology of the conglomerate channel belt depositional system. For location see Fig. 3.

marly background sediment. The conglomerates reveal a strikingly high percentage (>90%; Schlunegger *et al.,* 1993) of sandstone clasts derived from the frontal Alpine flysch units (Gasser, 1967). Associated medium- to coarse-grained sandstones generally measure a few centimetres in thickness and can be traced laterally over a few metres only. Mapping reveals that this unit encroaches large conglomerate fans (Fig. 3).

Interpretation

The geometry of the conglomerates suggests deposition in narrow ribbon-like channels which occupied stable positions over prolonged periods as indicated by the multistorey arrangements (see also Allen *et al.,* 1983). The lack of pebble lags, moderate sorting, rare stratification, the absence of a fine-grained matrix, the presence of outsized clasts and deep longitudinal furrows suggest deposition by turbulent hyperconcentrated flows on alluvial fans (Pierson, 1980). Beyond the intersection point between the mountain front and the fan, sheet floods developed and deposited thin, inversely graded conglomerate sheets in very shallow braided channel courses. The fine-grained background sediment documents a wide range of depositional processes from mudflows depositing mudstones with scattered pebbles to sheetfloods which deposited laminated mudstones and rippled sandstones and siltstones. This depositional system is assigned to the bajada because (i) it encroaches laterally on large fans (Fig. 3), (ii) the strikingly high percentage of clasts derived from the frontal Alpine units indicates a local sediment source and (iii) the occurrence of highly turbulent flows as well as mudflows suggests ephemeral, proximal discharges (see also Johnson *et al.,* 1986; Singh *et al.,* 1993).

Conglomerate Channel Belt depositional system

Conglomerates are the most abundant lithofacies of this unit. It measures up to 2 km in thickness and forms lens-shaped geometries in cross-sectional view with a lateral extent measuring up to 15 km (Figs 3 and 4). The conglomerates consist of single 1.5–5-m-thick units, which can be traced laterally for at least 250 m. Amalgamation of single conglomerate beds is common and results in 10–15-m-thick and more than 1-km-wide sheets. The conglomerates are clast supported and massive with occasional trough cross-beds. They have a strong concave shaped erosive base with deep scours (up to 1.5 m), some of which are marked by gutter casts. Low-angle 'epsilon' cross-beds, which dip at right angles to the gutter casts, are also present. The conglomerates are generally overlain by 2–12-m-thick fining-upward sandstones topped by siltstones and mudstones (Fig. 4). These fine-grained sediments display plane-lamination, ripple cross-lamination, mottling, root traces and bioturbation.

Interpretation

The geometry and texture of the individual conglomerate beds suggest deposition in fluvial channels. Epsilon cross-bedding indicates lateral migration of side-bars during waning floods, whereas massive bedding is the result of longitudinal bar construction between braided branches (Miall, 1978; Rust, 1978). This depositional system represents an environment with coarse-grained sinuous to braided channels bordered by floodplains.

Sandstone Channel Belt depositional system

A variety of lithofacies are observed in this ≤2-km-thick depositional environment (Fig. 5). Most abundant are medium- to coarse-grained sandstones, which occur as simple or amalgamated 5–10-m-thick units with a lateral extent ranging from 150 to 1500 m. They show an erosive base with rip-up clasts or a pebble lag. Towards the top, they gradually fine-up into overlying lithofacies. The sandstones are generally massive, but occasionally medium-scale trough-cross-beds and epsilon cross-beds are observed. Other units include fine- to medium-grained lenticular as well as tabular massive sandstones, climbing rippled siltstones and mottled mudstones.

Interpretation

These lithofacies correspond to the intermediate-scale architectural elements defined in the Aquitanian Plateau Molasse by Platt & Keller (1992). They were interpreted by these authors as meander channel sandstones, crevasse channel and crevasse splay sandstones, levee sandstones and siltstones and overbank fines and palaeosols.

Floodplain depositional system

Alternating mudstones and siltstones occur in units ranging in thickness from 100 to 400 m (Fig. 6). The generally massive mudstones are strongly mottled with abundant slickensides, bioturbation and rootcasts. Caliche nodules, colour stratification and occasionally vertical blocky fabrics also occur. The 10–20-cm bedded siltstones display climbing ripple cross-lamination, slumping, bioturbation and mottling. Rare ≤3-m-thick massive sandstone channels are also present (Fig. 6).

Interpretation

The extensive development of mottling, slickensides and colour stratification is characteristic of palaeosols and indicate repeated wetting and drying. The geometries and sedimentary structures of the sandstones and siltstones are indicative of levee, crevasse channel and crevasse

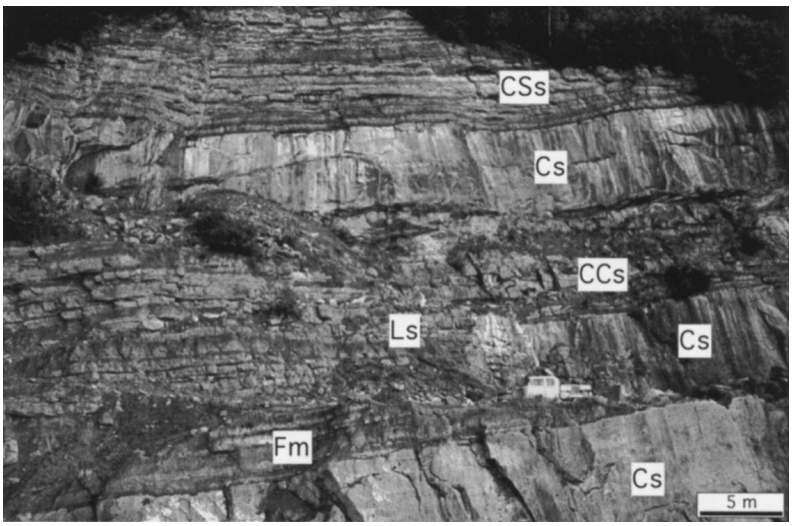

Fig. 5. Details of the sandstone channel belt depositional system showing the intermediate-scale architectural elements of Platt & Keller (1992). Cs: channel sandstone, CCs: crevasse channel sandstone, CSs: crevasse splay sandstone, Ls: levee siltstone, and Fm: floodplain mudstone. For location see Fig. 2.

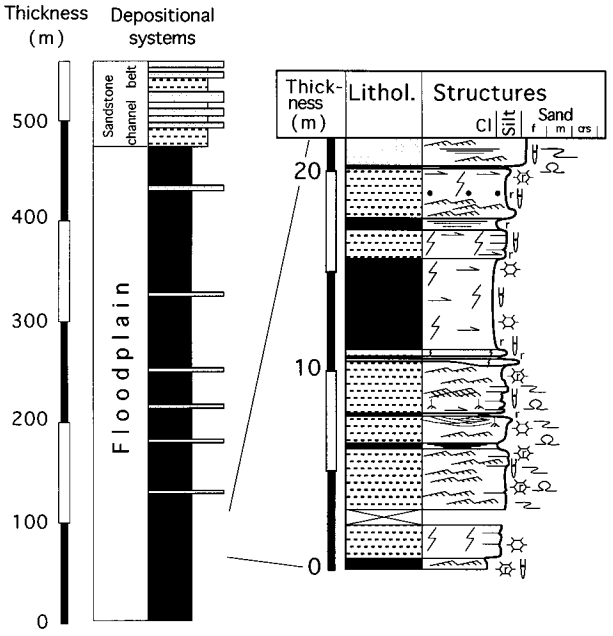

Fig. 6. Sedimentology of the floodplain depositional system. For location see Fig. 3, and for legend see Fig. 4.

splay deposits described by Platt & Keller (1992). Their association with abundant mudstones with pedogenic overprint is characteristic of the floodplain depositional system.

Lacustrine depositional system

This architectural element measures between 50 and 400 m in thickness and occurs both in a clastic and in a carbonate facies. Most widespread are 2–3-m-thick coarsening-upward sequences of laminated silty mudstones, laminated and rippled fine-grained sandstones capped by bioturbated and mottled silty fine-grained sandstones. Some 2–3-m-thick interbedded fine-to medium-grained sandstones and 20-cm-thick rippled siltstones also occur. Less abundant are up to 70-m-thick alternations of 0.5–6-m-thick micritic limestones and 0.5–2-m-thick calcareous organic-rich mudstones (Fig. 7). The carbonates contain ostracods, charophytes and gastropods and display caliche nodules, circumgranular cracks, glaebules and microkarst.

Interpretation

Both the small-scale mudstone–sandstone and the carbonate-dominated facies are interpreted as shallowing-upward lacustrine to palustrine cycles (Platt & Keller, 1992; Blaser *et al.*, 1994). The interbedded sandstones and siltstones are characteristic of crevasse channels, crevasse splays and levees deposited in shallow lakes as described by Platt & Keller (1992).

Seismostratigraphy

The concept of seismostratigraphy applied to sedimentary environments has proven helpful for reconstructing the

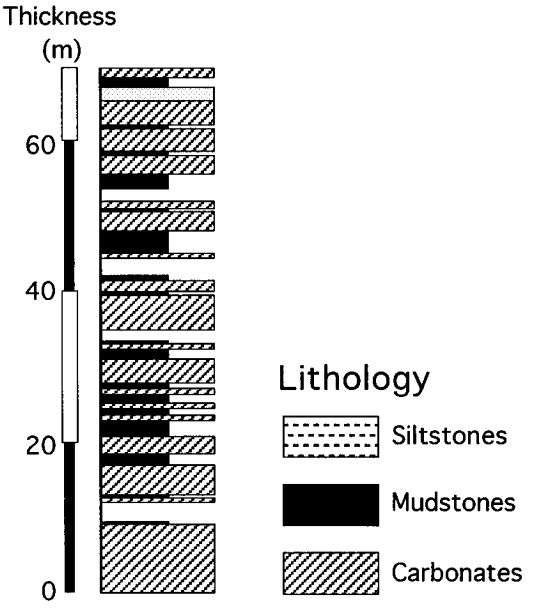

Fig. 7. Sedimentology of the lacustrine depositional system. For location see Fig. 2 (Brochene Fluh section).

geometry and the evolution of sedimentary sequences and depositional systems (Cross *et al.,* 1993; Prosser, 1993; Jin, 1995). It characterizes the seismic reflections in terms of lengths, amplitudes, frequencies and continuity which determine the seismic facies. These in turn are an expression of the large-scale lithological architecture of the subsurface referred to as depositional systems. The origin of architectural elements of this magnitude is, as outlined above, mainly controlled by extrinsic factors such as tectonics, climate and sea-level changes. Any large-scale change of these parameters will cause a rearrangement of the depositional systems, which is expressed in seismic sections by changes in bedding geometries or discordant relations which delimit sedimentary sequences.

Two seismic lines, running across the Plateau Molasse in a N–S (line 8307) and an E–W (line 8406) direction (Figs 2 and 8), have been analysed. The N–S line crosses the whole central Swiss Plateau and links the wells Hünenberg-1, Boswil-1 and Schafisheim, located in the southern, middle and northern part of the Plateau Molasse, respectively. Line 8406 is calibrated by the deep borehole Altishofen-1 and intersects with line 8307 at right angles near Boswil-1 (Fig. 2).

The base of the Tertiary Molasse fill is readily identified by a high-amplitude, low-frequency wave-group with a high continuity representing the surface of the gently southward dipping Mesozoic basement (Figs 8 and 9). In addition, the base Tertiary unconformity can be recognized on the N–S line by the discordance between the underlying Mesozoic reflectors and the overlying northward onlapping reflections.

The Molasse is highly reflective, although numerous reflections are discontinuous, indicating limited lateral extent of the beds. The boundaries between USM/OMM and OMM/OSM are detected by strong reflections, truncation in the underlying group and onlap of the succeeding unit (Figs 9 and 10).

Sedimentary sequences

Within the USM four depositional sequences (A–D) are identified (Figs 9–11). Sequence A, which is best developed in the N–S section (Fig. 9), comprises the oldest deposits of the southern part of the Plateau USM and extends as far as 5 km north of Boswil–1. It has a maximum thickness of 500 m in the Hünenberg-1 section, from where it thins to 350 m in the Boswil-1 section 10 km further north (Fig. 12). The basal reflections of sequence A onlap northward on the Mesozoic. The top of sequence A is defined by truncation of reflections and onlap of younger deposits (Figs 10A and 11). In the E–W section (Fig. 8B), sequence A thins from Boswil-1 to Altishofen-1, reaching a thickness of <200 m (Fig. 12).

Sequence B comprises the thickest unit of the Lower Freshwater Molasse in the studied area, measuring 750 m at Hünenberg-1 and *c.* 250–350 m at Boswil-1 and Altishofen-1 (Fig. 12). In the N–S section, it thins northward, reaching a minimum thickness of *c.* 200 m south of Boswil-1, and then thickens again reaching 400 m further north. The thickness variations are mainly due to an erosional relief with a relatively elevated area at km 5–12 (Fig. 9). Onlap on both flanks succeeded by overlap reflection indicate gradual blanketing of sequence A (e.g. Fig. 10A). The top of sequence B is defined by an extended high-amplitude low-frequency reflector, on which reflections of the overlying sequence C onlap northward (Fig. 9).

Sequence C comprises a relatively thin succession, measuring between 250 m in the Hünenberg-1 section and *c.* 200 m in the Boswil-1 and Altishofen-1 wells (Fig. 12). Upper and lower boundaries are best developed in the N–S line by onlap reflection terminations at its base and by reflection truncations at km 6–10 at its top (Fig. 10C). The relationships of reflections reveal that 0.5 s of the seismic section are missing south of km 10, which corresponds to an undecompacted sedimentary thickness of $\approx$200 m. In the E–W line, the upper boundary of sequence C is poorly constrained because no truncation and onlap terminations of reflections occur. Some eastward onlap terminations of reflections, however, are detected at the base of sequence C 5 km west of Altishofen-1 (Fig. 8B). Sequence D comprises the youngest deposits of the Lower Freshwater Molasse Group. Upper and lower boundaries are well constrained in the N–S line by onlap reflection terminations at its base and by reflection truncations at its top between km 4 and 7 (Fig. 10C, D). These truncations define the basal Burdigalian unconformity (Fig. 10D). In the E–W seismic section, no truncation of reflections occurs between USM and OMM, and a depositional hiatus separates both groups (Fig. 8).

Adding 100 m of strata eroded prior to the Burdigalian transgression at Hünenberg-1 (Schlunegger *et al* ., 1996a), the depositional thickness of sequence D was $\approx$400 m at Hünenberg-1 and *c.* 300 m at Boswil-1, suggesting a small taper of the USM of that time.

Seismic facies

Four seismic facies are identified in the N–S running seismic section 8307 (Fig. 13). Seismic facies 1 is characterized by laterally continuous (>1 km), parallel-bedded reflections with high-amplitude and low-frequency reflections. This seismic facies is present from 1800 to 2750 m in the well Hünenberg-1 (Fig. 12). It consists of alternating $\leq$15-m-thick, coarse-grained sandstones and mudstones corresponding to the sandstone channel belt depositional system. The high continuity of the reflections is indicative of widespread sheet sandstones with a width of up to 4 km (Fig. 9) suggesting deposition in channels which migrated across their floodplains. The large lateral extent of the sandstones together with their

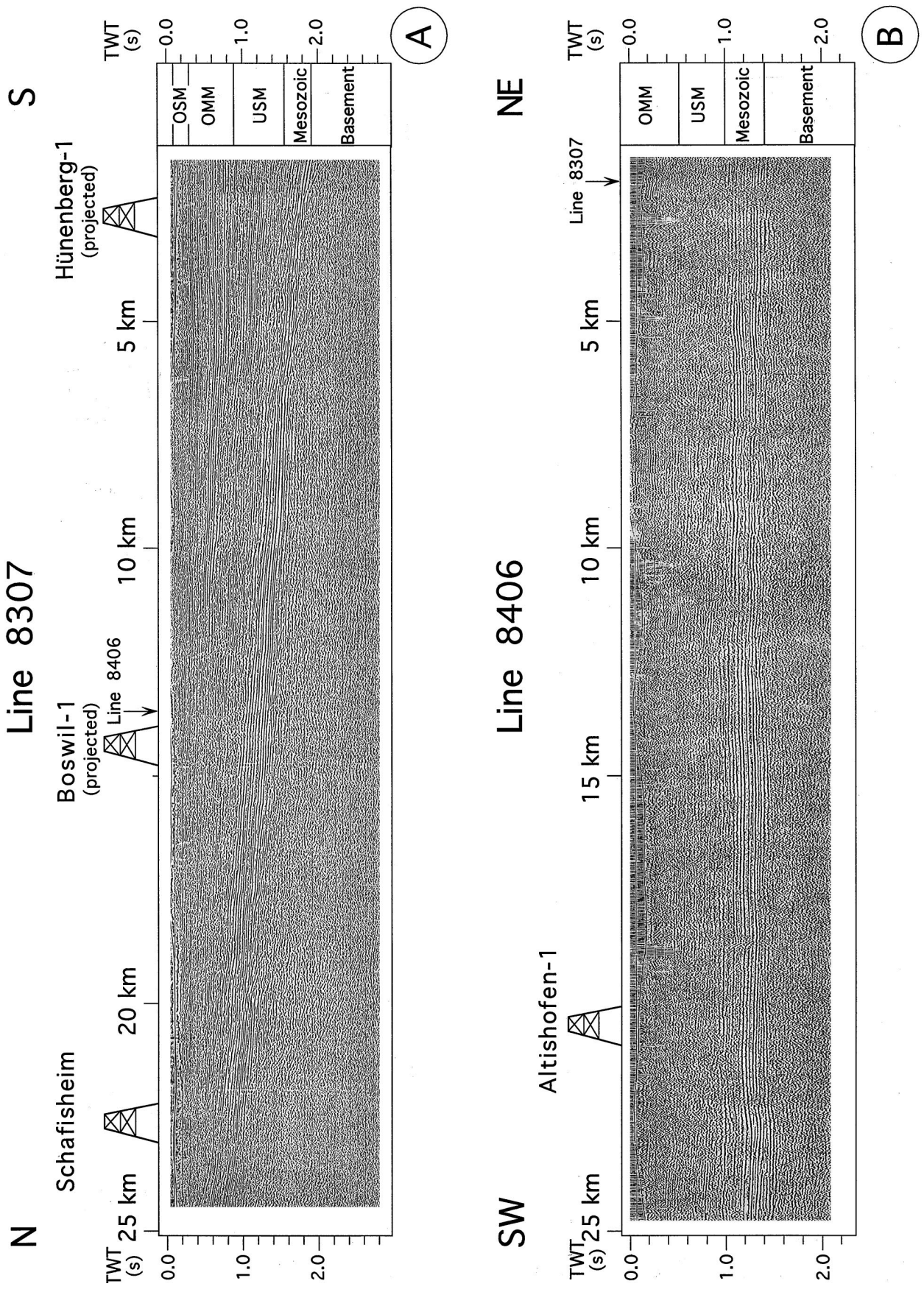
N
S
Line 8307
Schafisheim
Boswil-1
(projected)
Line 8406
Hünenberg-1
(projected)
TWT (s)
0.0
1.0
2.0
25 km
20 km
10 km
5 km
OSM
OMM
USM
Mesozoic
Basement
A
SW
NE
Line 8406
Altishofen-1
Line 8307
15 km
10 km
5 km
25 km
OMM
USM
Mesozoic
Basement
B

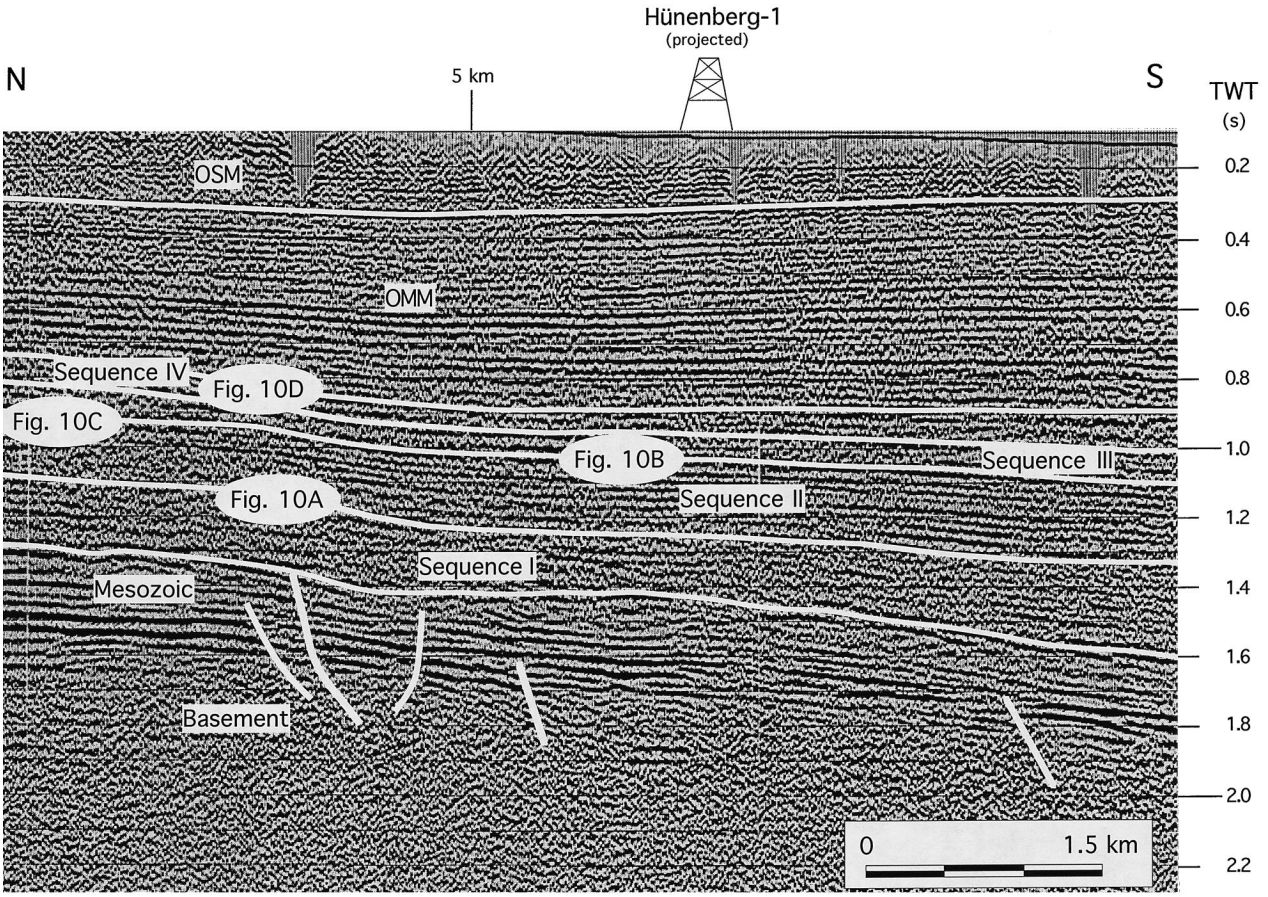

Fig. 9. Proximal part of the N–S seismic section (line 8307). See Fig. 10 for further details.

thickness, coarse grain size and high sandstone/mudstone ratio suggest a sand-dominated sedimentary environment characterized by multistorey bedload channels.

Seismic facies 2 is characterized by predominance of 200–400-m-wide, high-amplitude, and low-frequency reflections (Fig. 13). This facies was encountered from 2750 to 3250 m in the Hünenberg-1 well (Fig. 12). It is made up of an alternation of medium- to coarse-grained sandstones and mudstones and is interpreted to represent the sandstone channel belt depositional system. However, in contrast to seismic facies 1, the length of reflections does not exceed 600 m. Furthermore, the high percentage of mudstones and siltstones found in the mudlogs and seen on the gamma ray and sonic logs suggests occurrence of thick overbank sequences as well as some mudstone layers in channel sandstone beds. This facies association together with the geometry of the channel sandstones suggests deposition either by laterally stable flows (Friend *et al.*, 1979) or by meandering rivers with moderate to high avulsion rates (Heller & Paola, 1996). The second interpretation appears more reasonable because meander belt sandstones bordered by thick overbank fines are exposed in the distal Aquitanian USM (Platt & Keller, 1992).

Seismic facies 3 is characterized by a chaotic reflection pattern (Fig. 13). This facies is calibrated in Boswil-1 between 800 and 1450 m, where 25–100-m-thick siltstone and mudstone alternations with interbedded <0.5-m-thick sandstones were encountered, representing the overbank deposits (Fig. 12). Additionally, some <5-m-thick sandstones also occur. They are interpreted to represent crevasse splay and crevasse channel sandstones. This facies association is assigned to the floodplain depositional system. The chaotic pattern is indicative of the limited lateral continuity of the intermediate-scale architectural elements.

Seismic facies 4 shows a generally transparent pattern of reflections, interbedded with parallel-bedded and also chaotic reflections with low amplitudes and high frequencies (Fig. 13). Because no well data are available to calibrate this facies, a sedimentological interpretation is rather speculative. Nevertheless, the seismic pattern is

Fig. 8. (A) Unmigrated N–S seismic section across the Plateau Molasse (line 8307), indicating location of the boreholes and showing surfaces which delimit the Molasse groups. For details see Figs 9 and 10. (B) Unmigrated E–W seismic section across the Plateau Molasse (line 8406). Note that the borehole Altishofen-1 is located on the seismic line. For detail see Fig. 11.

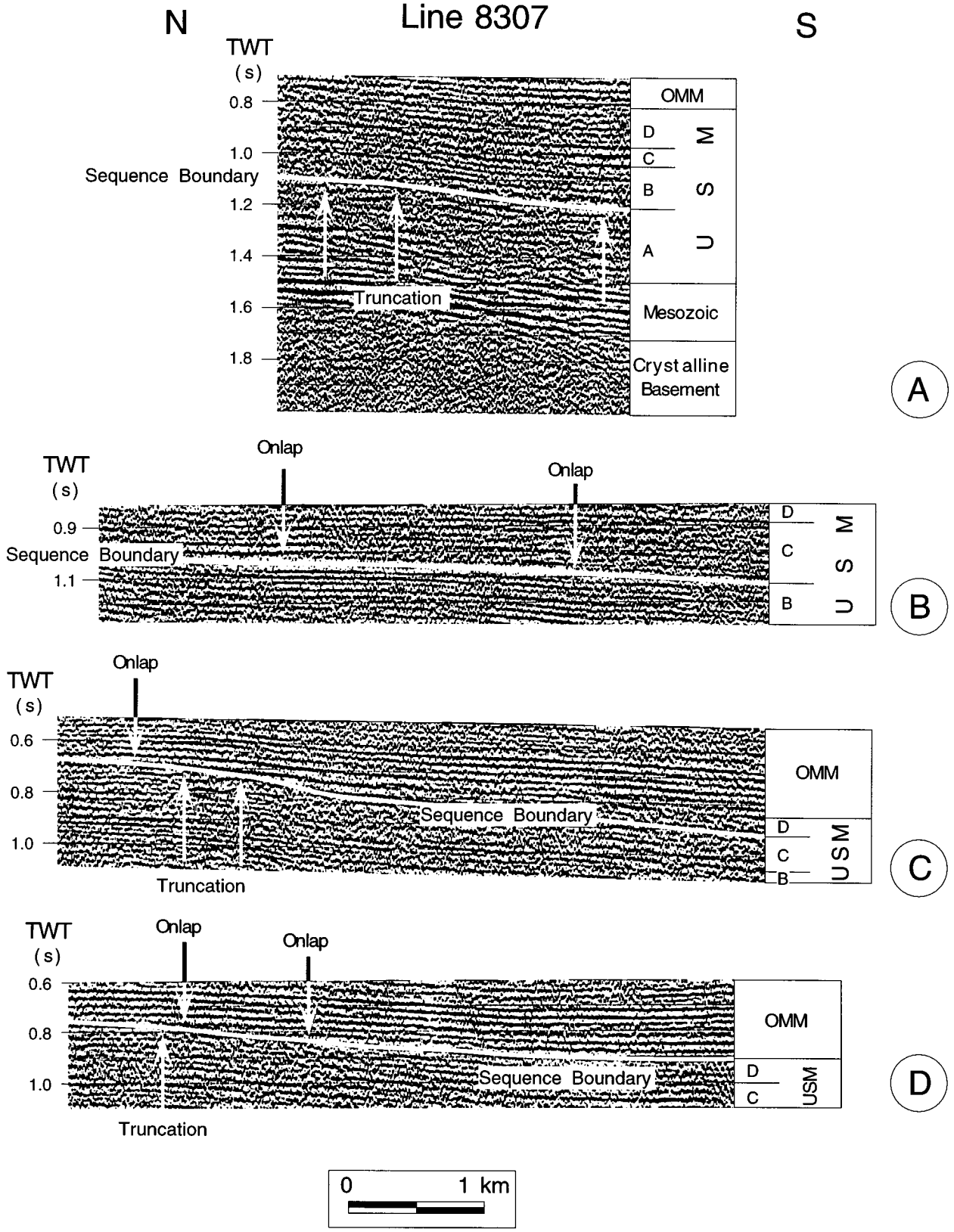

Fig. 10. Details from line 8307, showing onlap and truncation of reflections which delimit (A): sequences A and B; (B): sequences B and C; (C): sequences C and D; (D): sequence D and OMM.

an expression of a generally thin-bedded monotonous facies, possibly representing the lacustrine depositional system or a distal floodplain. Furthermore, the sedimentological evaluation of a core drilled 25 km north-east of Boswil-1 revealed the presence of abundant shallowing-upward lacustrine cycles in a distal floodplain

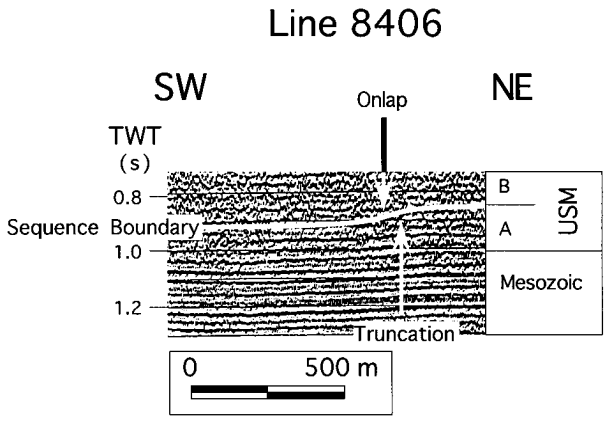

Fig. 11. Details from line 8406, showing truncation and onlap of reflectors which delimit sequences A and B. See Fig. 8 for location.

environment (Blaser *et al.*, 1994). Therefore, we tentatively assign seismic facies 4 to the lacustrine depositional system.

Facies relationships

Mapping of the seismic facies on the N–S seismic line allows reconstruction of the evolution of the depositional systems (Fig. 14). Multistorey bedload channels preferentially occur in the more proximal part of the basin, whereas meander channel belts, floodplain and lacustrine environments occupied the more distal northern part of the basin. Two phases of progradation are recorded in the Lower Freshwater Molasse Group (Fig. 14). The first starts with a sandstone meander belt system in sequence A and evolves into a northward expanding system of multistorey channel belts during sequence B, reaching the area of Boswil-1. The occurrence of seismic facies 3 at the base of sequence B 1 km north of Hünenberg-1, however, indicates the presence of a floodplain bordered by multistorey bedload channels. This facies relationships suggests that the area north of Hünenberg-1 experienced less subsidence than the adjacent areas during the initial phase of sequence B. The

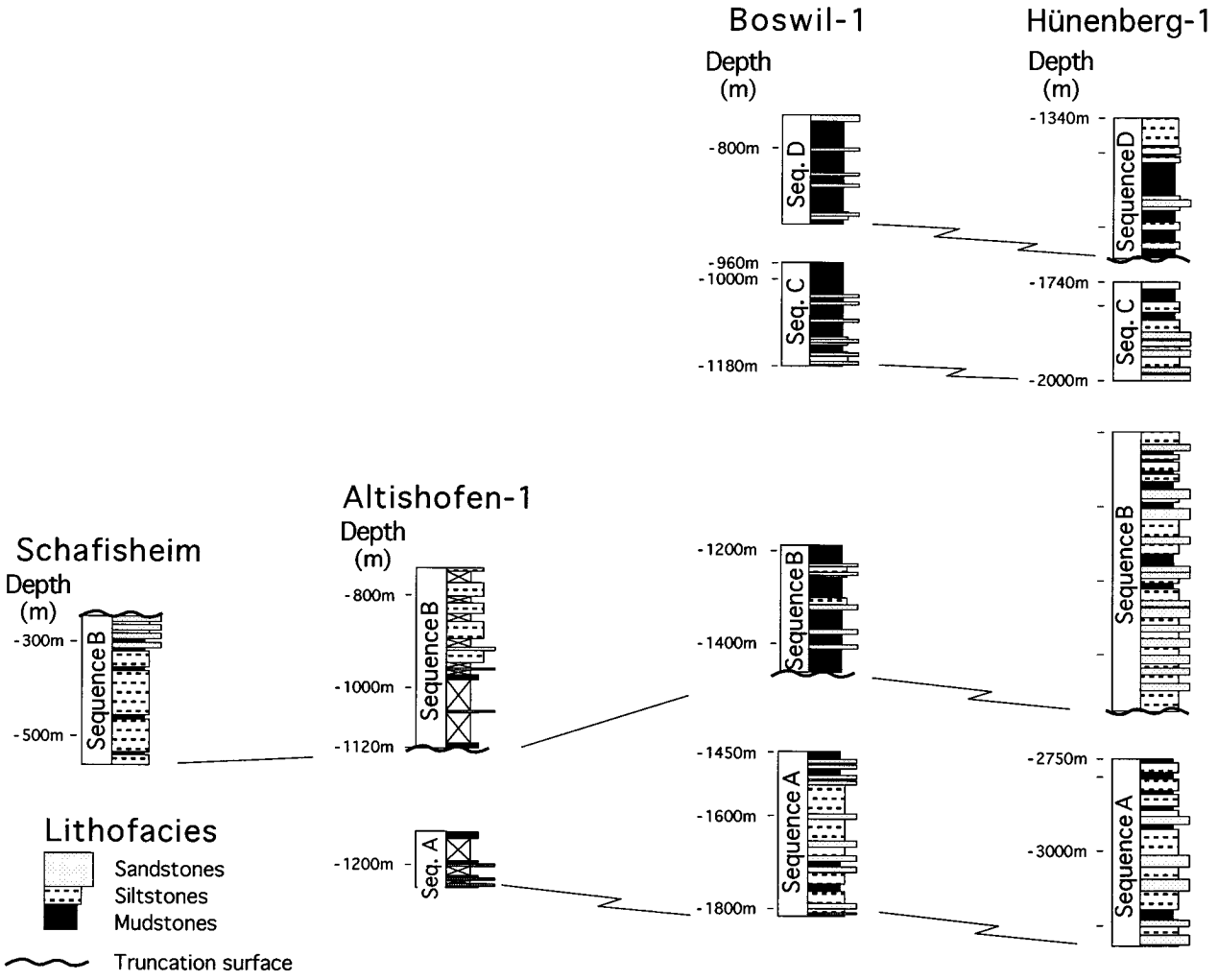

Fig. 12. Lithological logs of the Hünenberg-1, Boswil-1, Altishofen-1 and Schafisheim sections, indicating strong variations in thicknesses of the sedimentary sequences. The lithologies are reconstructed based on cores, mudlog information and geophysical data using the methodology described in detail by Blaser *et al.* (1994). The sections were divided into sedimentary sequences based on the seismic data shown on Figs 9–11.

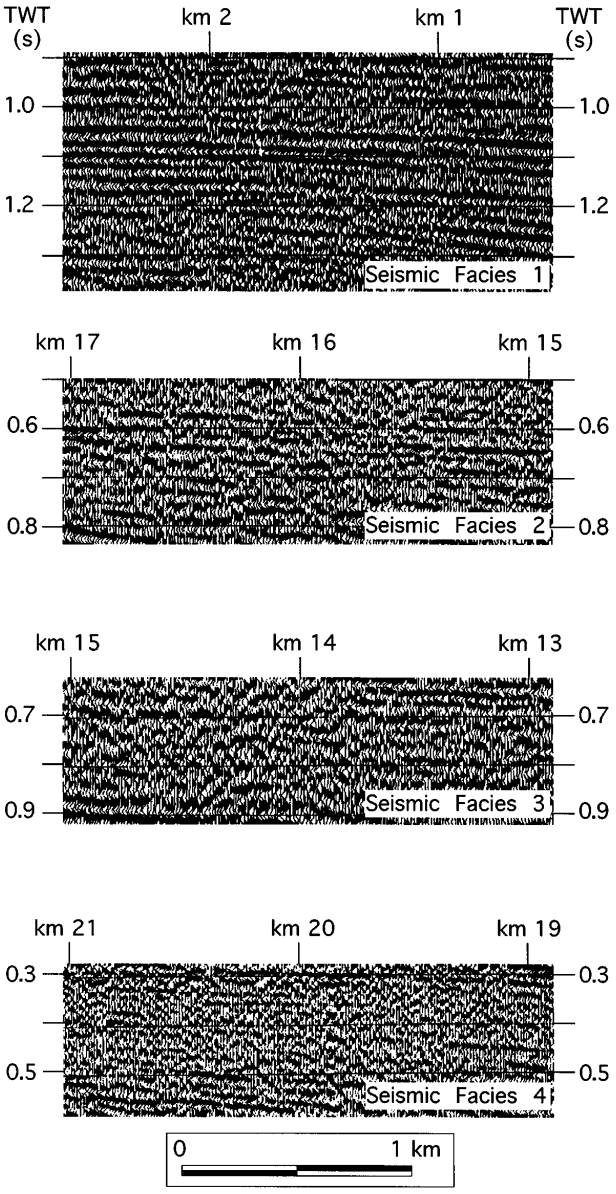

Fig. 13. Details from line 8307 showing the characteristics of the four seismic facies. Note that the difference in TWT between the horizontal lines is 0.1 s, and that the width of the figures represents 2 km.

second progradational phase comprises sequences C and D, during which the system of multistorey channel belts expanded northward from km 7 to 12. The lacustrine depositional system located at the distal basin edge of the basin, however, did not shift further north despite the northward progradation of the sandstone channel belts.

Chronostratigraphy

The success of magnetostratigraphy in the Swiss Molasse lies in its applicability to every depositional system, provided that mudstones and siltstones are present, and in its high temporal resolution (Burbank *et al.,* 1992; Schlunegger *et al.,* 1996a, b). The chronological framework of the Lower Freshwater Molasse of the studied cross-section is reconstructed using the magnetostratigraphic calibration of the Brochene Fluh section located at the feather edge of the basin 20 km west of the studied transect (Fig. 2, Schlunegger *et al.,* 1996a). The ages of the uppermost 800 m at Hünenberg-1 were assessed projecting the magnetostratigraphic chronologies of the Fischenbach section (Fig. 2) into the studied transect. This correlation is justified because time-equivalent strata are of equal thickness in the Fischenbach area (Schlunegger, 1995). In addition, new chronologies are established on cores of the wells Weiach and Altishofen-1.

The relatively high sample density of the Weiach and Altishofen sections allows definition of a sufficiently well-constrained reversal pattern (Fig. 15). Except for R2 of the Weiach section, all magnetozones of both sections are defined based on at least one class I and one class II site. The magnetic polarity stratigraphy (MPS) of the Weiach section is characterized by nine magnetozones. The correlation to the magnetic polarity time scale (MPTS) of Candy & Kent (1992, 1995; Fig. 16) is guided by (i) mammalian index fossils of MN1 at the top of the Weiach section (Matter *et al.,* 1988a, b), (ii) calibration of MN1 with chrons 6Br to 6AAr.2 by Schlunegger *et al.*(1996a) and (iii) a distinct pattern of reversals characterized by a thick interval of normal polarity at the top of the section underlain by relatively short intervals of normal and reversed polarities (Fig. 15). This suggests a correlation with chrons 6Cr to 6AAr.3 or 6AAr.2 of the MPTS (Fig. 16). This correlation implies that the very short reversed polarity in chron 6Bn and possibly the normal polarity in chron 6AAr. 2 were missed due to a low sample density. The correlation of the Altishofen MPS with the MPTS, however, is more difficult because of a hiatus separating sequences A and B. Nonetheless, sequence A may be correlated with chrons 9n to 8n because mammal sites indicate MP26 for the base of the USM immediately south of the Jura Mountains (Fig. 2 of Engesser, 1990) and because MP26 was calibrated with chrons 9n to 7r (Schlunegger *et al.,* 1996a) (Fig. 16). The upper part of the Altishofen MPS comprises sequence B. A one-to-one correlation of this part of the Altishofen MPS with chrons 7r to 6Bn of the MPTS (Fig. 16) is constrained by the absence of seismic unconformities (Fig. 8b), suggesting continuous accumulation of sediment, and by a remarkable petrographic change with a sudden increase of epidote (Maurer *et al.,* 1982) at the base of the normal polarity interval N3 (Fig. 15). This event was dated at *c.* 25.5 Ma (Schlunegger *et al.,* 1996a) and found to be contemporaneous in the Subalpine thrust belt and the Plateau Molasse 50 km further west (Schlunegger *et al.,* 1993). It appears, however, that the very short reversed polarity in chron 7n.1 was missed because of a low sample density. The Brochene Fluh section, representing the lowermost USM at the feather-edge of the basin, spans chrons 6Cr to 6Cn.2r according to Schlunegger *et al.* (1996a), i.e. 24.5–23.8 Ma (Fig. 16).

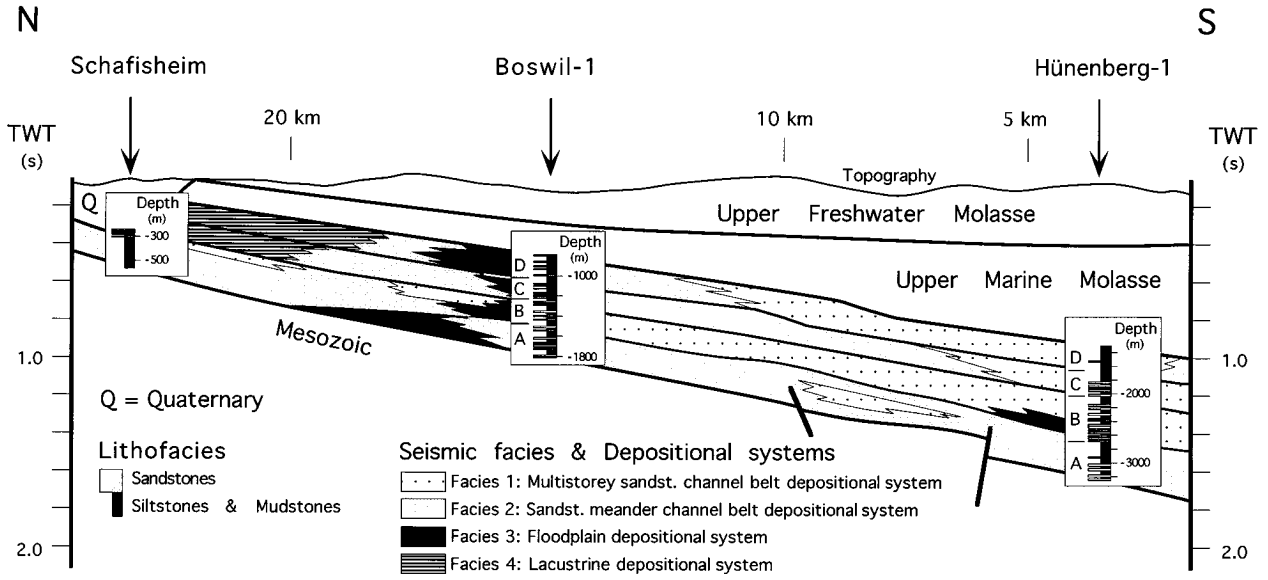

Fig. 14. Facies relationships of the Lower Freshwater Molasse based on the sedimentological interpretation of the seismic lines calibrated by the neighbouring boreholes.

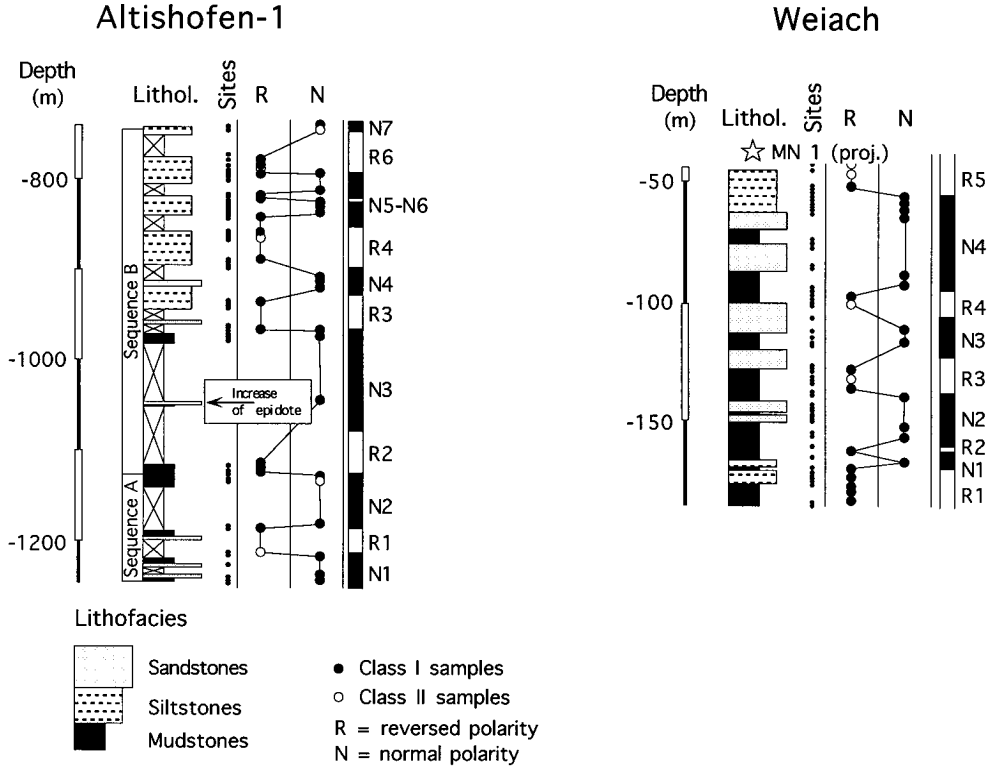

Fig. 15. Magnetostratigraphy of the Althishofen-1 and Weiach sections. The definition of the reversal pattern is based on measured inclinations of the samples and the statistically tested (Fisher, 1953) consistencies of inclinations and rotated declinations, which qualify the magnetic sites as class I and II.

At the southern margin of the Plateau Molasse, however, the deposition of the Lower Freshwater Molasse began at *c.* 28 Ma (base of sequence A, see also calibration of the Altishofen section) and lasted up to 20.5 Ma according to Schlunegger *et al.* (1996a).

The magnetic calibrations of these sections allow reconstruction of the facies relationships and the two progradational cycles in a detailed temporal framework (Fig. 17). Sequence A comprises the time interval between 28 and 26 Ma, whereas the hiatus separating sequences A and B spans *c.* 1–2 Myr. Sequence C lasted from 23 to 22.3 Ma in the southern part of the Plateau Molasse and from 23 to *c.* 22 Ma further north. Sedimentation of D began as early as 21.5 Ma in the Hünenberg-1 area and $\approx$0.5 Myr later in the northern part of the basin. Here, however, the absence of significant

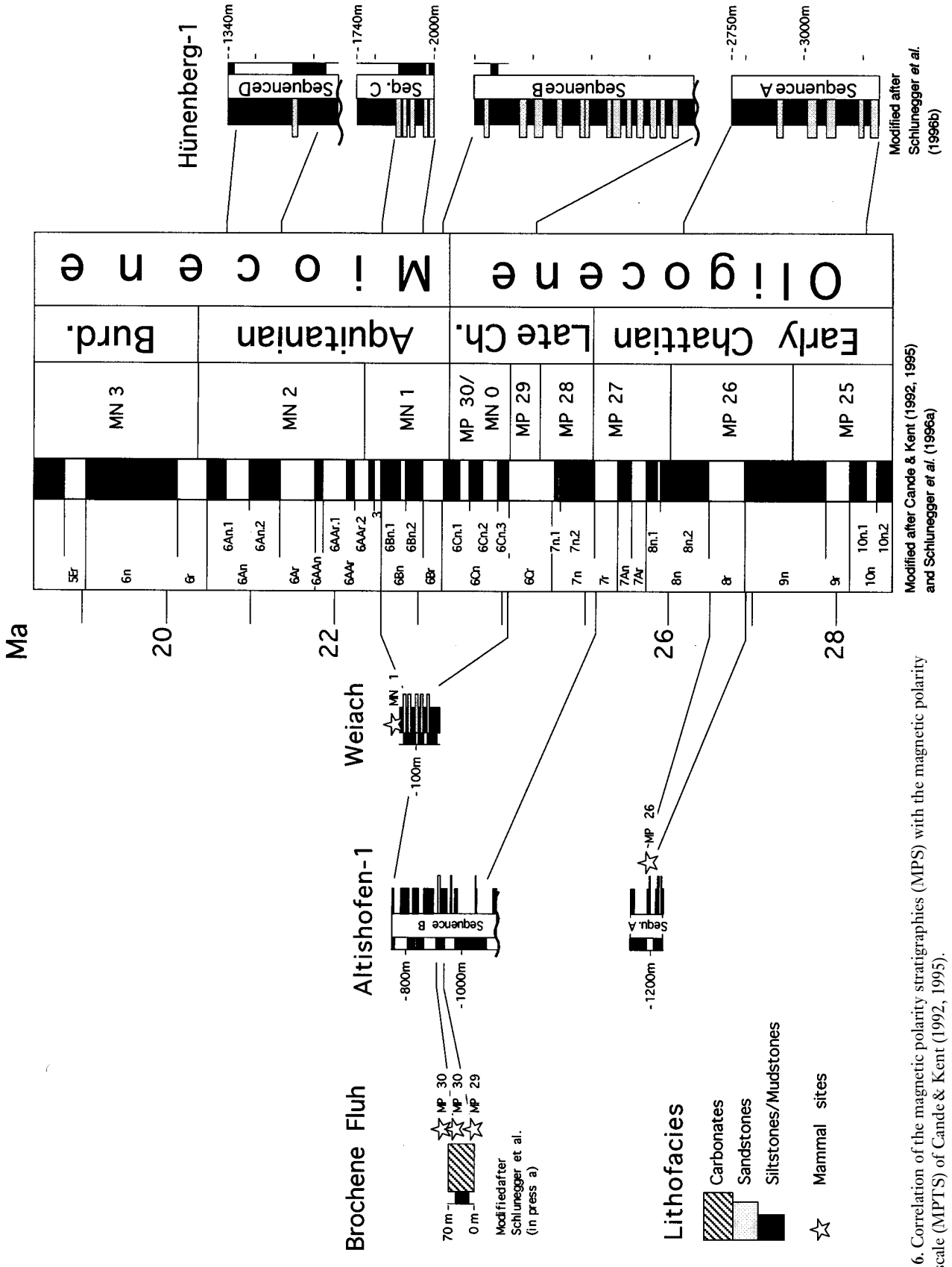

Fig. 16. Correlation of the magnetic polarity stratigraphies (MPS) with the magnetic polarity time-scale (MPTS) of Cande & Kent (1992, 1995).

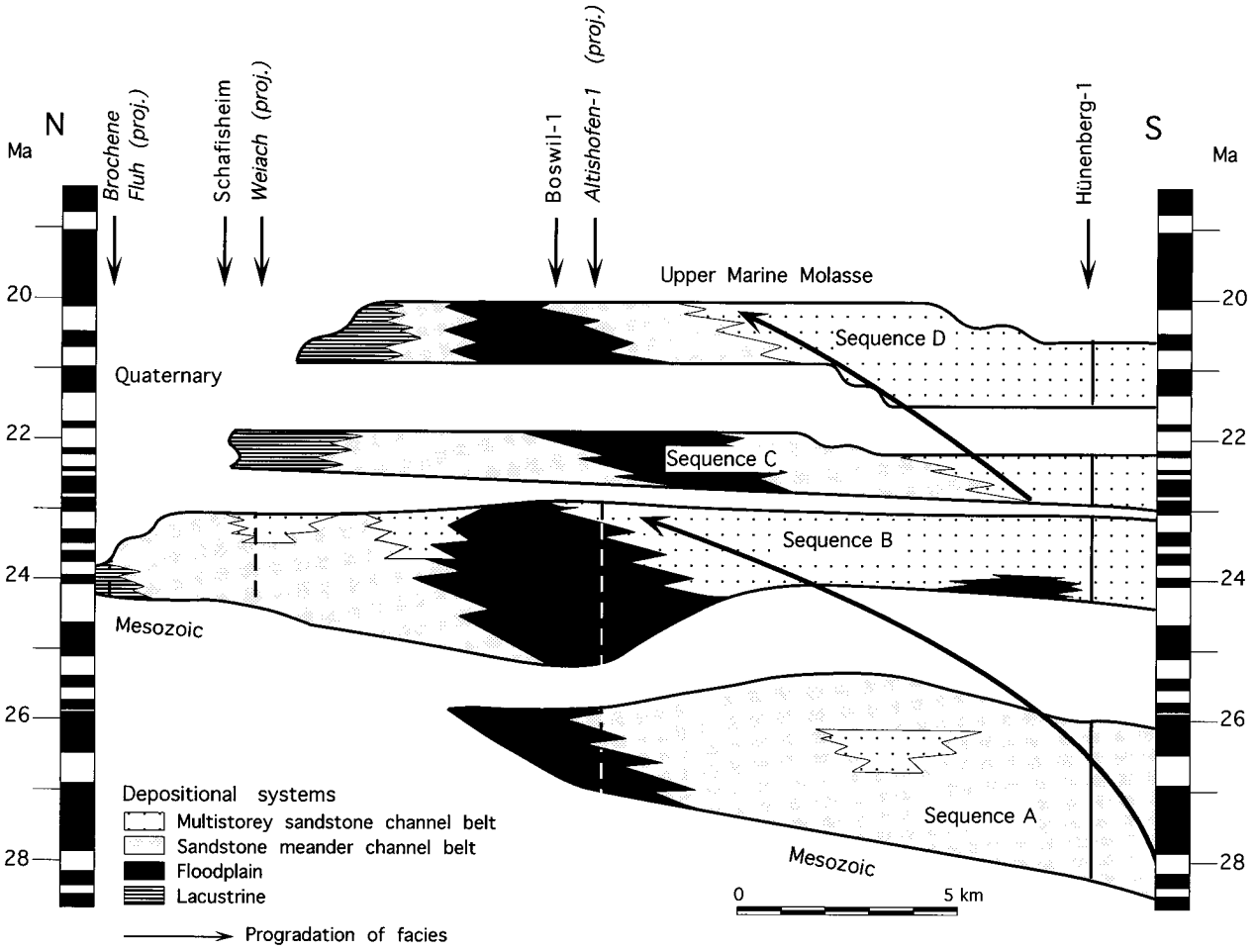

Fig. 17. Wheeler diagram of the studied Lower Freshwater Molasse showing heterochroneity of facies and the two progradations of the multistorey sandstone channel belt depositional systems from the proximal to the distal part of the basin.

erosion during the Burdigalian transgression results in an upper age limit for sequence D of *c.* 20 Ma, as opposed to 20.5 Ma in the southern part.

Dispersal systems

The various lithofacies of the studied transect are the product of a broad spectrum of depositional processes ranging from channellized flows to unconfined flows in overbank areas. Four major dispersal systems (Honegg, Höhronen, Napf, Lac Léman) are identified based on the distribution of characteristic heavy mineral associations (Figs 18 and 19). The deposits of the first alluvial system, referred to as the Honegg system, comprise the 28–26-Ma-old succession of sequence A. The sandstones are characterized by occurrence of the key heavy minerals apatite and zircon as well as by a high carbonate content (Schlunegger *et al.,* 1993; Schlunegger, 1995). The depocentre of the Honegg system was located 50 km south-west of the study area, from where the Honegg river drained north-eastward into the study area (Schlunegger, 1995). However, occurrence of traces of spinel detected at the base at Hünenberg-1 suggests some admixtures of the Rigi dispersal system (Schlunegger *et al.,* 1996b), the depocentre of which was located at the Alpine front immediately south of the analysed transect (Stürm, 1973). The second major alluvial system, called the Höhronen system, was active between 24.5 and *c.* 22.3 Ma and is characterized by the key heavy minerals apatite and zircon as well as abundant crystalline clasts in the conglomerate population (Kleiber, 1937; Füchtbauer, 1959; Gasser, 1966; Müller, 1971; Schlanke, 1974). Its depocentre was located west of the fan apex of the Rigi river, from where it drained eastward into the analysed cross-section (Schlunegger *et al.,* 1996b). In the studied transect, the deposits of the Höhronen river system constitute sequences B and C south of Boswil-1 (Fig. 18 and 19). The increasing abundance of epidote from sequence C to D, however, suggests progressive establishment of the third system, referred to as the Napf system (Füchtbauer, 1959, 1964; Matter, 1964; Gasser, 1966). Mapping and sedimentological studies reveal that the depocentre of the Napf river was located 30 km south-west of the studied transect and that it covered an area of >600 km^2 (Schlunegger, unpublished data). From there it drained north-eastward as revealed by heavy mineral data (Füchtbauer, 1959, 1964).

Traces of blue amphibole and hornblende characterize

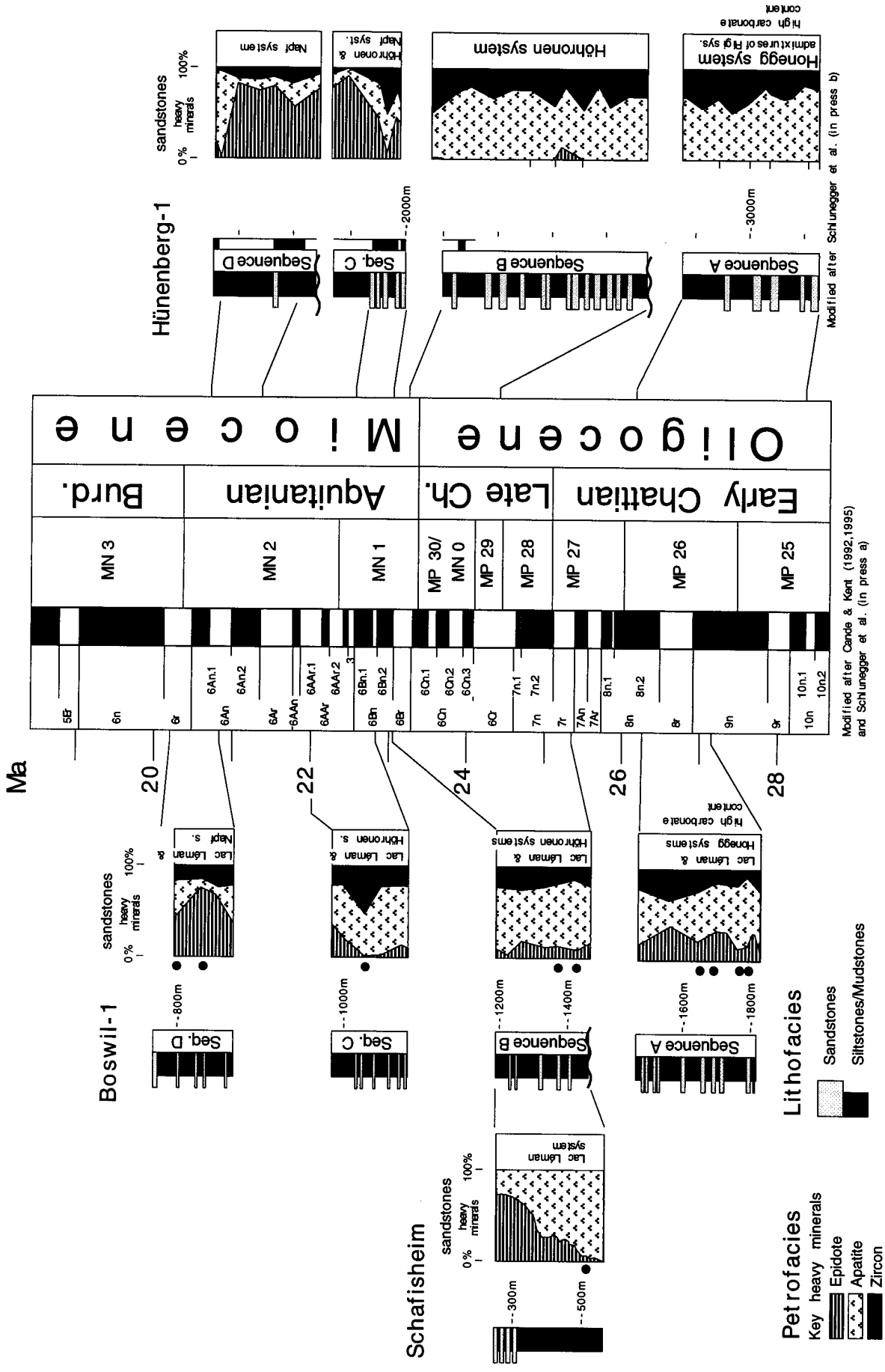

Fig. 18. Petrography of the Lower Freshwater Molasse in the detailed temporal framework.

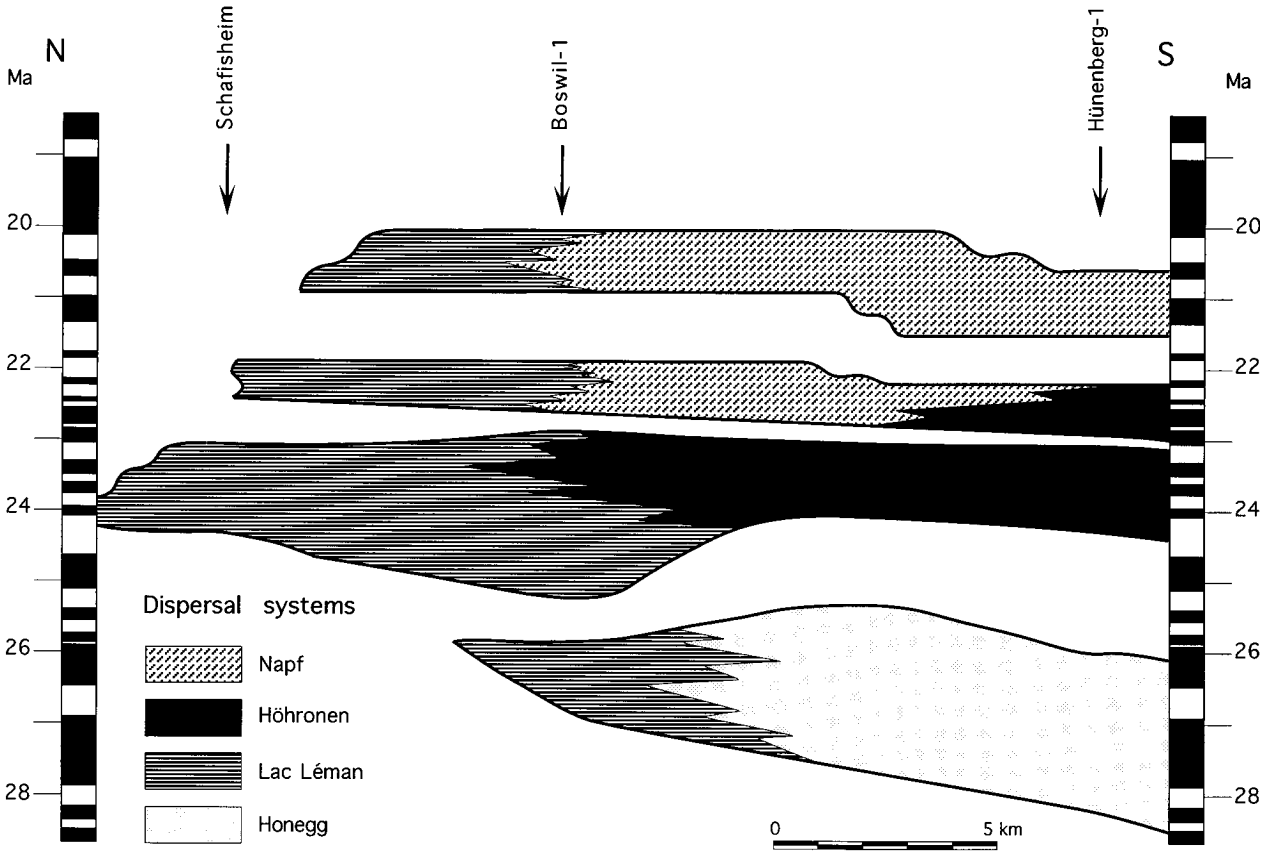

Fig. 19. Wheeler diagram, revealing the temporal and spatial distribution of the dispersal systems.

the Lac Léman system (Maurer *et al.,* 1982). The depocentre of this system was located at the western end of the Molasse Basin ≈150 km south-west of the study area. From there it discharged eastward to the study area (Schlanke *et al.,* 1978; Maurer *et al.,* 1982). The presence of these heavy minerals in the USM of the wells Boswil-1 and Schafisheim (Fig. 18) suggests that this axial system occupied the Molasse Basin from its northern margin to the Boswil area (Fig. 19).

DISCUSSION

As pointed out above, the Molasse Basin fill is divided into the mainly flat-lying Plateau Molasse and that found in a thrust belt which crops out in the Subalpine zone. Because of the different outcrop conditions the reconstruction of the basin-fill history of the USM was achieved by outcrop studies in the proximal Subalpine Molasse (Schlunegger *et al.,* 1996b) and subsurface investigations in the Plateau Molasse using seismic and borehole data. Correlation of the two domains is achieved by high-resolution magnetostratigraphy and by palinspastic restoration of the Subalpine sections (Schlunegger *et al.,* 1996b). In the following section the evolution of the USM basin is depicted by four time slices. They reveal that the basin architecture is a function of the basin geometry and the subsidence pattern, which in turn evolved in response to orogenic events in the Alpine hinterland (Fig. 1).

As discussed by Schlunegger *et al.* (1996b), synmagmatic backthrusting along the Insubric Line (Fig. 1) (Schmid *et al.,* 1989, 1996) and enhanced erosional denudation in the southern central orogen (Hurford, 1986; Giger & Hurford, 1989) as well as forward thrusting at the tip of the orogenic wedge (Calanda phase of deformation, Milnes & Pfiffner, 1977, 1980) coincides with the first stage of the evolution of the USM between 30 and 25.5 Ma. During that time, the Molasse Basin formed a *c.* 50-km-wide wedge-shaped basin with a high flexural angle at the Alpine thrust front, reaching maximum values of 6–7° (Schlunegger *et al.,* 1996b) (Fig. 20a). Magnetostratigraphies established at Rigi (Schlunegger *et al.,* 1996b) and seismic data reveal a progressive northward progradation of the basin fill and a continuous decrease of the angle of unconformity between the Molasse strata and the Mesozoic basement (Figs 17 and 20A), indicating an increase in the sediment supply/accommodation space ratio. At the Alpine front, the basin fill consists of a >3600-m-thick, coarsening- and thickening-upward sequence comprising a floodplain, conglomerate channel belt, alluvial megafan and bajada depositional system from the base to the top. Further north beyond the site Entlebuch-1, however, no coarsening- and thickening-upward sequence developed, and a <500-m-thick sequence of alternating sand-, silt- and mudstones was deposited by meandering rivers in the *c.* 23-km-wide distal northern part of the basin.

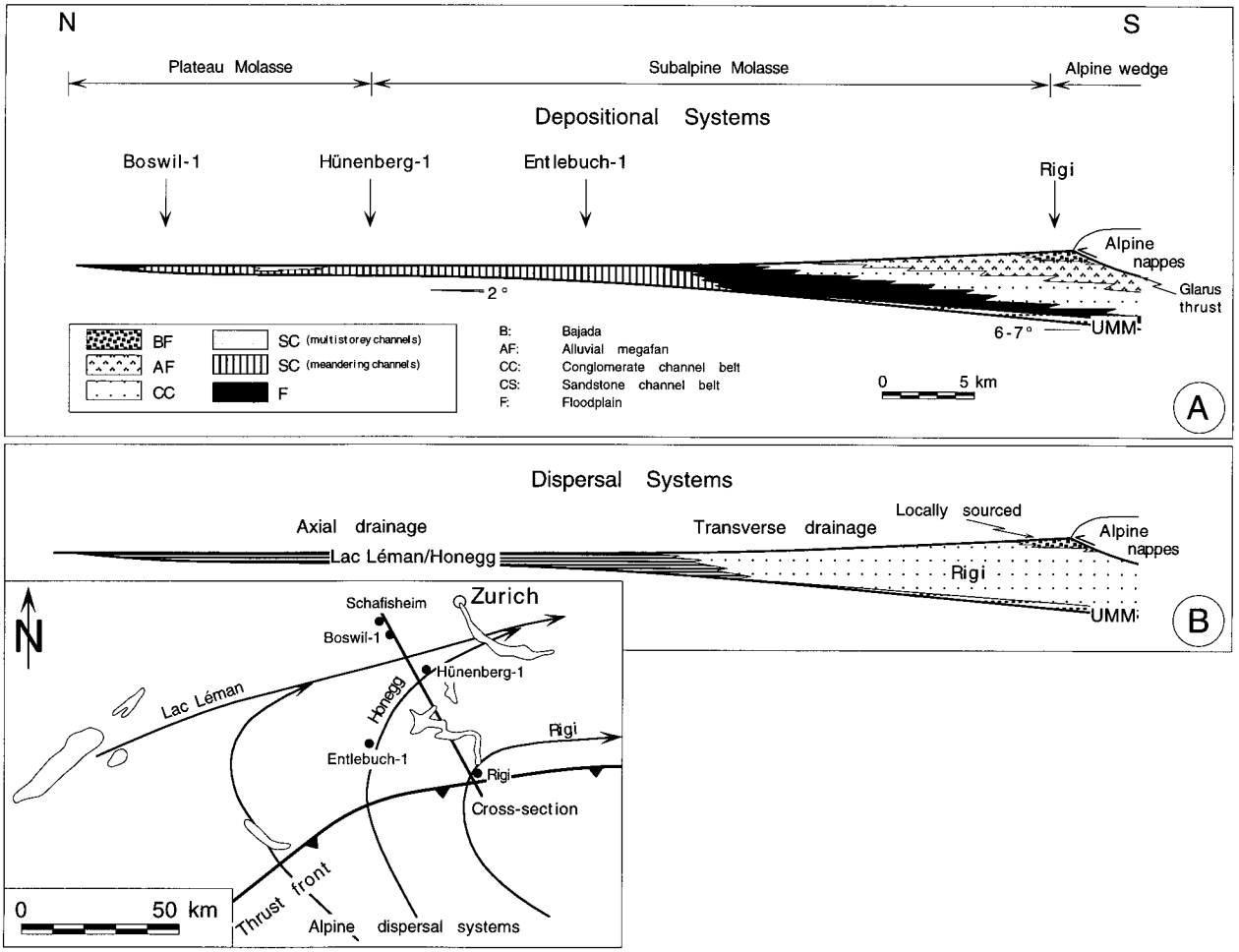

Fig. 20. Palaeogeographical diagram for the time interval between 30 and 25.5 Ma, showing the basin geometry and architecture (A) as well as the location of the dispersal systems (B).

Here, the flexural dip of the basement was *c.* 2° (Schlunegger *et al.,* 1996b), suggesting relatively low lateral gradients of basin subsidence. This first phase of basin formation is succeeded by a basin-wide unconformity, during which at least 300 m of lower Chattian strata was removed by erosion (Figs 8, 9 and 10A). During the first phase of USM basin formation, the narrow trough adjacent to the Alpine front was filled by the transverse Rigi dispersal system as shown by the occurrence of the key heavy minerals spinel, zircon and apatite as well as the predominance of carbonate clasts in the conglomerate population (Figs 18 and 20B; Stürm, 1973). In the distal reaches of the basin, however, predominance of the axial systems derived from further west indicates that the Rigi system did not expand across the area of increased flexure (Fig. 20B).

The formation of the wedge-shaped basin geometry with enhanced flexure at the tip of the Alpine wedge is interpreted as the result of forward thrusting along the Glarus thrust (Fig. 1) in the early Oligocene (stable sliding of the entire wedge). This interpretation is supported by (i) cross-cutting relationships between calibrated metamorphic fabrics, suggesting slip along the Glarus thrust in the early Oligocene (Milnes & Pfiffner, 1977, 1980), (ii) an increasing admixture and size of clasts derived from the frontal Flysch nappes in the proximal Molasse, indicating uplift and enhanced erosion of the Alpine front (Schlunegger *et al.,* 1996b) and (iii) numerical models of orogen/foreland basin systems that reveal an increase in the basin subsidence at the thrust front as a result of thrust front propagation (Flemings & Jordan, 1989, 1990; Sinclair *et al.,* 1991). The increase in the sediment supply/accommodation space ratio associated with the coarsening- and thickening-upward trend at Rigi appears to be the result of enhanced erosional denudation rates in the source area of the Rigi river. Indeed, cooling ages from the upper Penninic and Austroalpine nappes of eastern Switzerland suggest high erosional denudation rates of >1 mm yr^{-1} in the Oligocene (Hurford, 1989; Giger, 1991).

Thrusting of the Helvetic thrust nappes above the Infrahelvetic complex along the Glarus thrust (Fig. 1) (Calanda phase of deformation) resulted in low-grade metamorphism in the latter units between 20 and 25 Ma (Frey *et al.,* 1980; Erdelbrock, 1994; Rahn *et al.,* 1994, 1995). Because thermal accommodation to new crustal loads lasts several million years (Werner, 1980; Schmid *et al.,* 1987), the Calanda phase of deformation was

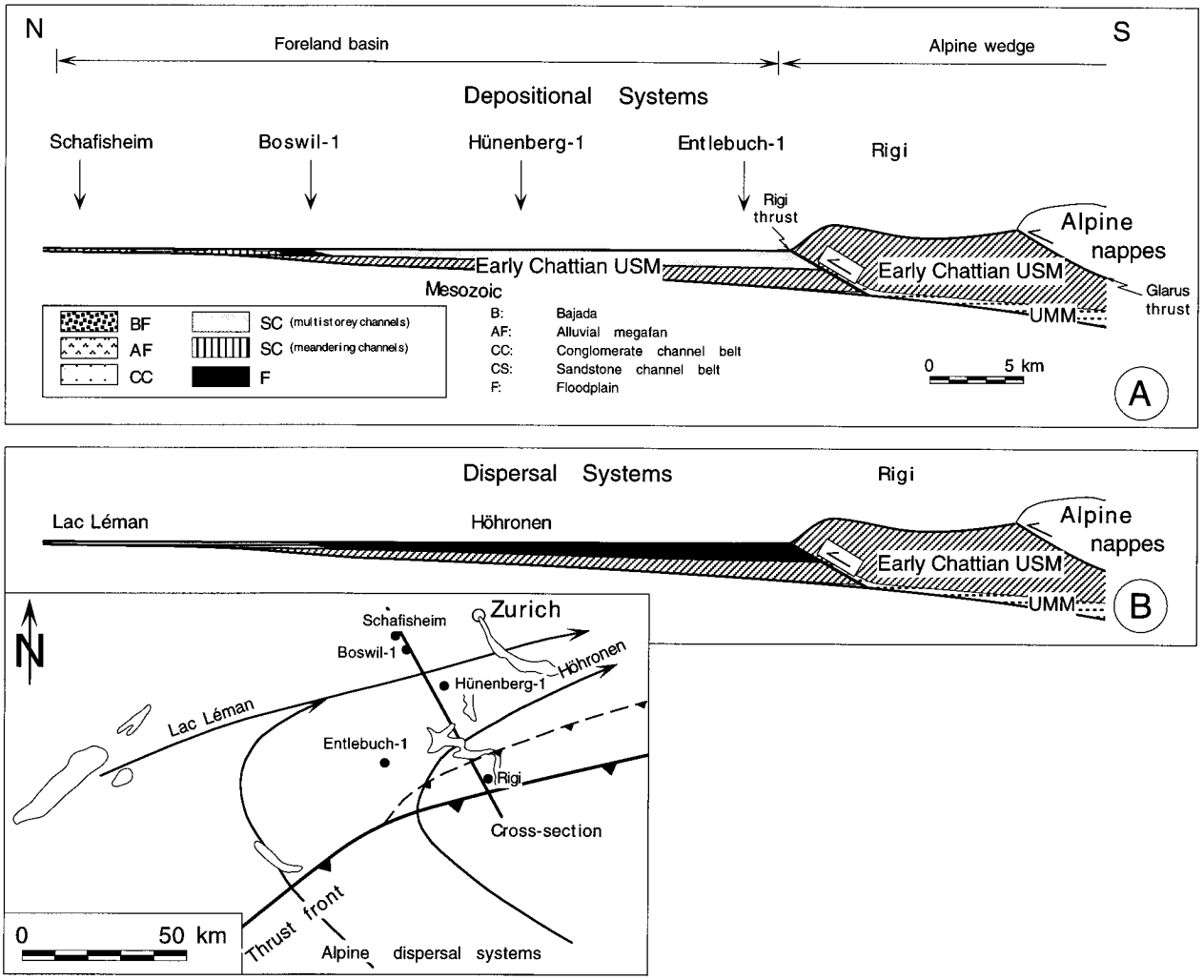

Fig. 21. Cross-section across the USM of central Switzerland at 23 Ma, showing the facies relationships (A) and the location of dispersal systems (B).

completed at the Oligocene/Miocene boundary. Therefore, cessation of slip movement along the Glarus thrust coincides with the erosional unconformity at the end of the first stage of USM basin formation, suggesting that uplift and erosion in the foreland was caused by an isostatic rebound of the crust.

Initial propagation of the Alpine thrust front into the foreland (activation of the Rigi thrust) coincides with the second stage of basin evolution between *c.* 24 and 23 Ma (Schlunegger *et al.,* 1996b). During that time, the proximal part of the Molasse was uplifted and eroded, and in the more distal reaches, the Molasse Basin formed a >35-km-wide, smoothly southward-dipping ($\approx 2°$), wedge-shaped basin (Fig. 21A). At Hünenberg-1, a 750-m-thick multistorey sandstone channel belt system deposited by the Höhronen river is present, whereas in the more distal northern part of the basin a 350-m-thick succession of meander belt sandstones and mudstones was deposited by the Lac Léman dispersal system (Fig. 21B). In contrast to the previous stage of basin evolution, the deposits of the Höhronen river expanded to the more distal reaches of the basin, suggesting an increase in the sediment supply/accommodation space ratio during that time. Initial incorporation of the proximal USM into the orogenic wedge represents an event of accretion at the toe of the wedge, as opposed to stable sliding of the entire wedge. Accretion simply redefined the leading edge of the wedge as being further onto the flexed plate. Therefore, no significant new loads would have been added above the flexed plate by this accretion. Thus, the shape of the flexural depression would not change, but the proximal edge of the depositional foreland would be shifted northward above more gently flexed crust (Fig. 21A).

The cross-section representing the stage III of USM basin evolution between 23 and 21.5 Ma shows incorporation of previously deposited 30–25.5-Ma-old alluvial megafan conglomerates into the tip of the orogenic wedge (Fig. 22A) (Schlunegger *et al.,*. 1996b). During that time, the Aar massif reached shallow crustal levels from initially 12 km at 25 Ma to *c.* 8 km at 20 Ma according to cooling ages and radiometric calibration of metamorphic minerals (Frey *et al.,* 1980; Hurford, 1986; Frey, 1988; Soom, 1990; Michalski & Soom, 1990; Pfiffner, 1996). This

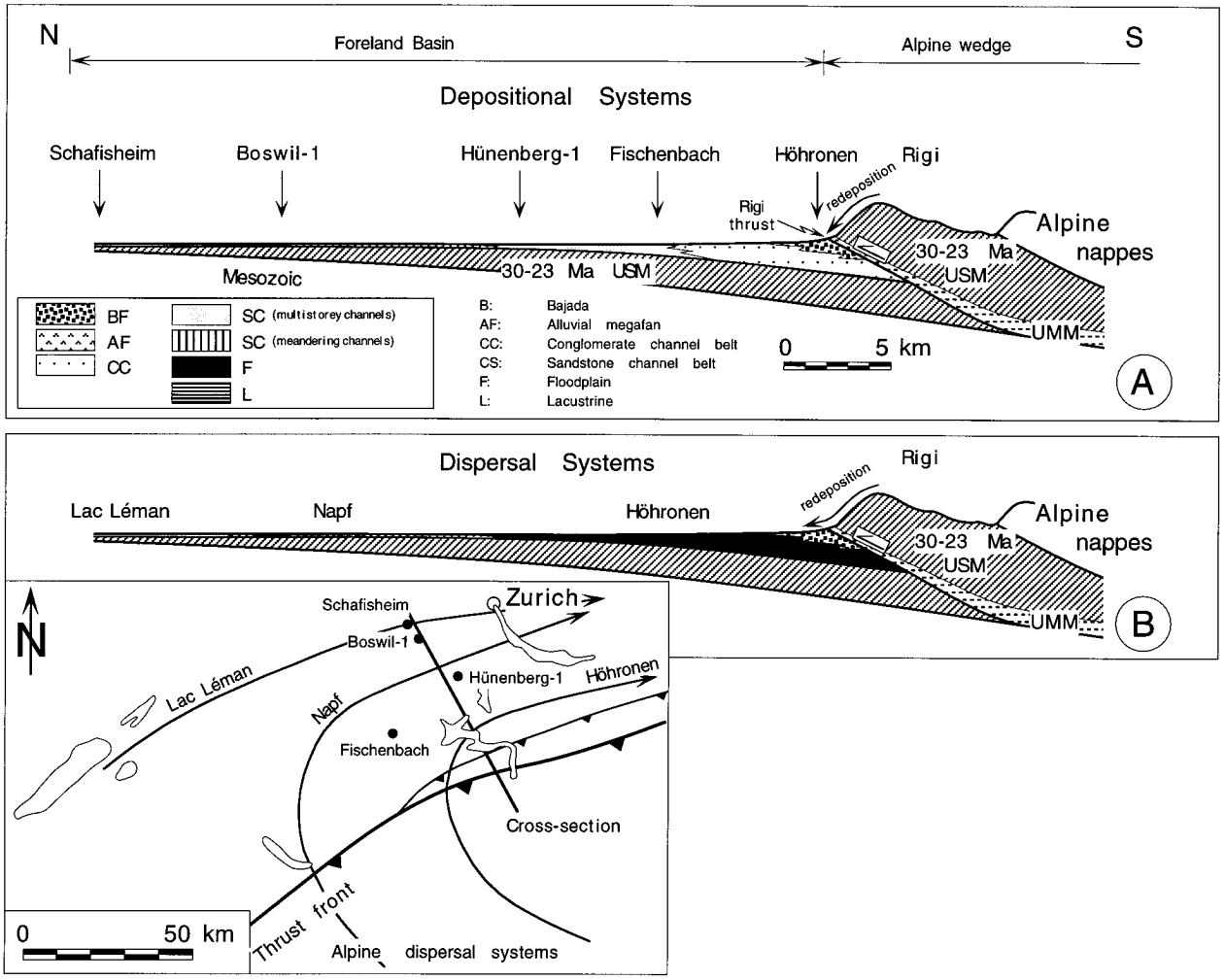

Fig. 22. Sketch figure showing the tectonostratigraphic configuration of the USM at 21.5 Ma (A) as well as the location of the dispersal systems (B). Note that the early Chattian conglomerates are uplifted and incorporated into the toe of the wedge.

phase of Alpine evolution coincides with the formation of a *c.* 15-km-wide trough south of the Fischenbach site (proximal sub-basin) and of a gently dipping ($\approx 1°$) >30-km-wide sub-basin in the distal reaches (Fig. 22A). The fill of the southern sub-basin consists of a coarsening- and thickening-upward sequence representing the conglomerate channel belt and bajada depositional systems, whereas in the northern part of the basin, the sandstone channel belt, floodplain and lacustrine depositional systems are present. Despite the change in basin geometry compared with the previous stage of Molasse evolution, the southern sub-basin remained occupied by the Höhronen river (Fig. 22B). In the northern distal reaches, the appearance of abundant epidote together with traces of blue amphibole and hornblende reveal the presence of the Napf dispersal system which mixed with the still-active Lac Léman system. However, only partial mixing between the systems of both sub-basins indicate that the Höhronen river did not expand across the area of the increased flexural angle.

At *c.* 21.5 Ma thrusting along the Rigi thrust was completed (Schlunegger *et al.*, 1996b). Cessation of slip movement along the Rigi thrust coincides with the erosional unconformity between the third and final stage of USM evolution, suggesting that uplift and erosion in the foreland was caused by an isostatic rebound of the crust.

Further exhumation of the Aar massif and forward thrusting and incorporation of previously deposited Molasse strata into the toe of the wedge coincides with the final stage of USM evolution at 21.5–20 Ma (Pfiffner *et al.*, 1996; Schlunegger *et al.*, 1996b). Because this phase of accretion redefined the leading edge of the wedge as being further north, the depositional foreland was shifted northward above more gently flexed crust. Furthermore, because this phase of accretion decreased the taper of the wedge, the topographic slope of the feeding river systems decreased, and predominantly channel belt sandstones were deposited in the southern part of the basin, while lacustrine mudstones prevailed in the distal foreland (Fig. 23A).

The Höhronen system was de-activated by this time (Fig. 23B). The predominance of epidote in the southern reaches of the basin, however, indicates deposition by

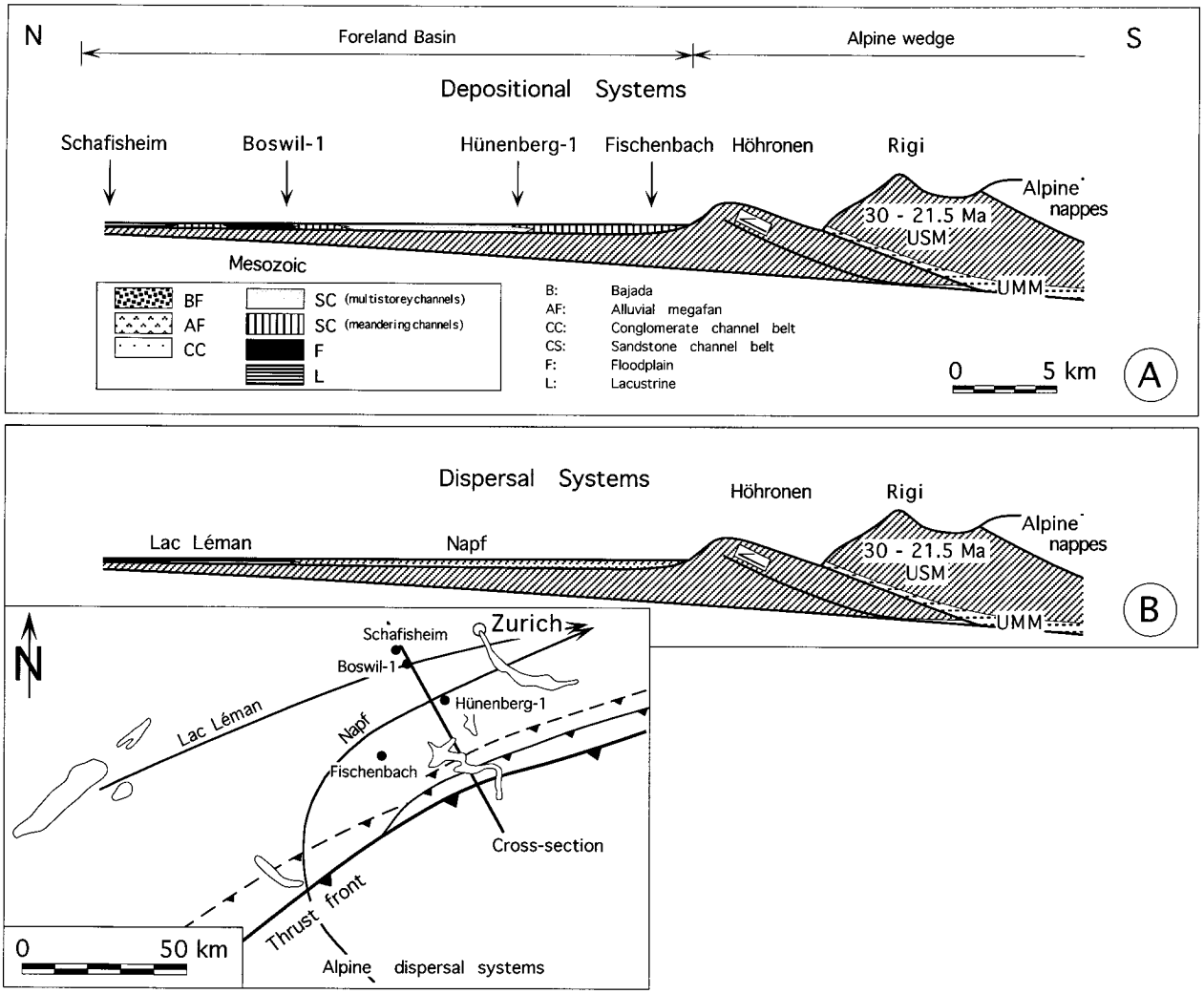

Fig. 23. Diagram revealing the tectonostratigraphic configuration of the USM at 20 Ma (A) and the location of the dispersal systems (B). Note that the USM reveals a low taper and that the triangle zone starts to form by initiation of a blind thrust (fault-propagation fold, see also Schlunegger *et al.*, 1996b).

the Napf river, whereas the Lac Léman system still occupied the northern distal portion of the basin as indicated by occurrence of blue amphibole and hornblende.

CONCLUSIONS

The combination of seismostratigraphy, sedimentary facies analysis, sedimentary petrography and magnetostratigraphy allows for the first time a detailed reconstruction of the evolution of the depositional history of the Lower Freshwater Molasse Group as a function of orogenic events. Petrofacies changes and coarsening-and thickening-upward sequences are related to the orogenic evolution of the Alpine hinterland.

Stable sliding of the entire wedge caused an increase in the crustal load at the tip of the orogenic wedge. As a result, two sub-basins were formed with different geometries. The proximal sub-basin attained a width of *c.* 20 km and a high flexural angle reaching maximum values between 6 and 7°. In contrast, a 30-km-wide smoothly dipping (<2°) sub-basin was formed in the more distal reaches of the foreland. Phases of accretion at the toe of the wedge redefined the leading edge of the wedge further onto the flexed plate. As a result, the depositional foreland was shifted northward above more gently flexed crust.

Stable sliding of the entire wedge succeeded by accretion at the toe of the wedge created progradational cycles which are represented in the proximal Molasse by a coarsening- and thickening-upward sequence followed by synsedimentary erosion. In the distal part of the basin the same trend is observed. However, it is strongly time transgressive: during development of the megasequence in the proximal sub-basin finer grained sediments with no recognizable trend were laid down in the distal sub-basin. However, subsequent uplift and erosion of the proximal basin fill (phase of accretion at the toe of the wedge) caused progradation of the depositional systems resulting in a coarsening- and thickening-upward megasequence in the distal basin (see also Fig. 17).

The reconstruction of the flexural response of the

basin to thrusting events, including basin wavelengths and subsidence rates, can serve to constrain elastic properties of the underlying crust as well as the thickness of the orogenic wedge. These data can be used to assess the relationships between crustal thickening and denudation of the orogen, which in turn allows estimation of the sediment flux into the basin (Schlunegger *et al.*, unpublished observation). As revealed by Sinclair *et al.* (1991), sediment flux, crustal rigidity and thrust loads and tectonic activity at the thrust front (stable sliding vs. accretion) are fundamental parameters which control the evolution of the North Alpine foreland basin.

ACKNOWLEDGMENTS

This project was carried out as part of the senior author's PhD project, with funding provided by the Swiss National Science Foundation (grant no. 21-36219.91). We would like to thank S. Lund for advice on interpreting the demagnetization data. Thanks go to H. Haas for the time-consuming heavy mineral separation, H. Bärtschi for technical instruction and S. Henyey for processing numerous magnetic samples. The help of S. Burns with the English is kindly acknowledged. Thanks go to the Natural Museum of Basel for providing the core of the Altishofen-1 well and to Swisspetrol for permission to publish line 8307 as well as the heavy mineral data of Boswil-1 and Hünenberg–1. Special thanks go to O. Kempf and P. Strunck for fruitful discussions. Finally, F.S. thanks his colleagues who acted as assistants and climbing instructors.

REFERENCES

Allen, P.A., Cabrera, L., Colombo, F. & Matter, A. (1983) Variation in fluvial style on the Eocene-Oligocene alluvial fan of the Scala Dei Group, SE Ebro Basin, Spain. *J. geol. Soc.*, 140, 133–146.

Anadon, P., Cabrera, L., Colombo, F., Marzo, M. & Riba, O. (1986) Syntectonic intraformational unconformities in alluvial fan deposits, eastern Ebro Basin margins (NE Spain). In: *Foreland Basins* (Ed. by P. A. Allen and P. Homewood), *Spec. Publ. Int. Ass. Sediment.*, 8, 259–272.

Baumberger, E. (1927) Die stampischen Bildungen der Nordwestschweiz und ihrer Nachbargebiete mit besonderer Berücksichtigung der Molluskenfaunen. *Eclogae geol. Helv.*, 20, 533–578.

Beaumont, C. (1981) The evolution of sedimentary basins on a visco-elastic lithosphere. Theory and examples. *Geophys. J. r. astron. Soc.*, 65, 291–329.

Beer, J.A., Allmendinger, R.W., Figueroa, D.E. & Jordan, T.E. (1990) Seismic stratigraphy of a Neogene piggyback basin, Argentina. *Bull. Am. Ass. Petrol. Geol.*, 74, 1183–1202.

Berli, S. (1985) Die Geologie des Sommersberges (Kantone St. Gallen und Appenzell). *Ber. St. gall. natf. Ges.*, 82, 112–145.

Blair, T.C. & McPherson, J.G. (1994a) Alluvial fan processes and forms. In: *Geomorphology of Desert Environments* (Ed. by A. D. Abrahams and A. J. Parsons), pp. 354–402. London, Chapman & Hall.

Blair, T.C. & McPherson, J.G. (1994b) Alluvial fans and their natural distinction from rivers based on morphology, hydraulic processes, sedimentary processes, and facies. *J. sedim. Res.*, A64, 451–490.

Blaser, P., Gubler, T., Küpfer, T., Marschall, P., Matter, A., Matyas, J., Meier, B.P., Müller, W.H., Schlanke, S., Schlunegger, F., Sieber, N. & Wyss, E. (1994) *Geothermiebohrung Bassersdorf, Charakterisierung der Oberen Meeresmolasse und Unteren Süsswassermolasse*. Nagra, Wettingen.

Bromley, M.H. (1991) Variations in fluvial style as revealed by architectural elements, Kayenta Formation, Mesa Creek, Colorado, USA. In: *The Three-Dimensional Facies Architecture of Terrigenous Clastic Sediments and its Implications for Hydrocarbon Discovery and Recovery* (Ed. by A. D. Miall and N. Tyler), *Spec. Publ. Soc. econ. Paleont. Miner., Concepts in Sedimentology and Paleontology*, 3, 94–102.

Büchi, U.P. & Schlanke, S. (1977) Zur Paläogeographie der schweizerischen Molasse. *Erdöl-Erdgas-Z.*, 93, 57–69.

Burbank, D.W. & Beck, R.A. (1991) Rapid, long-term rates of denudation. *Geology*, 19, 1169–1172.

Burbank, D.W., Beck, R.A Raynolds, R.G.H., Hobbs, R. & Tahirkheli, R.A.K. (1988) Thrusting and gravel progradation in foreland basins: a test of post-thrusting gravel dispersal.*Geology*, 16, 1143–1146.

Burbank, D.W., Engesser, B., Matter, A. & Weidmann, M. (1992) Magnetostratigraphic chronology, mammalian faunas, and stratigraphic evolution of the Lower Freshwater Molasse, Haute-Savoie, France. *Eclogae geol. Helv.*, 85, 399–431.

Burbank, D.W., Raynolds, R.G.H. & Johnson, G.D. (1986) Late Cenozoic tectonics and sedimentation in the northwestern Himalayan foredeep: II. Eastern limb of the northwest syntaxis and regional synthesis. In: *Foreland Basins* (Ed. by P. A. Allen and P. Homewood), *Spec. Publ. Int. Ass. Sediment.*, 8, 293–306.

Cande, S.C. & Kent, D.V. (1992) A new geomagnetic polarity timescale for the late Cretaceous and Cenozoic. *J. geophys. Res.*, 97, 13917–13951.

Cande, S.C. & Kent, D.V. (1995) Revised calibration of the geomagnetic polarity timescale for the Late Cretaceous and Cenozoic. *J. geophys. Res.*, 100, 6093–6095.

Cross, T.A., Baker, M.R., Chapin, M.A., Clark, M.S., Gardner, M.H., Hanson, M.S., Lessenger, M.A., Little, L.D., McDonough, K.J., Sonnenfeld, M.D., Valasek, D.W., Williams, M.R. & Witter, D.N. (1993) Applications of high-resolution sequence stratigraphy to reservoir analysis. In: *Subsurface Reservoir Characterization from Outcrop Observations* (Ed. by R. Eschard and B. Doligez), pp. 11–33. Proc. 7th Explor. Res. Conf., Paris, Technip.

Diem, B. (1986) die Untere Meeresmolasse zwischen der Saane (Westschweiz) und der Ammer (Oberbayern). *Eclogae geol. Helv.*, 79, 493–559.

Erdelbrock, K. (1994) *Diagenese und schwache Metamorphose im Helvetikum der Ostschweiz 'Inkohlung und Illit-'Kristallinität'*. PhD thesis, University of Bern.

Fisher, R.A. & (1953) Dispersion on a sphere. *Proc. r. Soc. London*, A217, 295–305.

Flemings, P.B. & Jordan, T.E. (1989) A synthetic stratigraphic model of foreland basin development. *J. geophys. Res.*, 94, 3851–3866.

Flemings, P.B. & Jordan, T.E. (1990) Stratigraphic modelling of foreland basins: interpreting thrust deformation and lithospheric rheology. *Geology*, 18, 430–434.

FREY, M. (1988) Discontinuous inverse metamorphic zonation, Glarus Alps, Switzerland: evidence from illit 'crystallinity' data. *Schweiz. Mineral. Petrogr. Mitt.*, 68, 171–183.

FREY, M., TEICHMÜLLER, M., TEICHMÜLLER, R., MULLIS, J., KÜNZI, B., BREITSCHMID, A., GRUNDER, U. & SCHWIZER, B. (1980) Very low-grade metamorphism in the external parts of the Central Alps: illite crystallinity, coal rank and fluid inclusion data. *Eclogae geol. Helv.*, 73, 173–203.

FRIEND, P.F., SLATER, M.J. & WILLIAMS, R.C. (1979) Vertical and lateral building of river sandstone bodies, Ebro basin, Spain. *J. Geol. Soc.*, 106, 36–46.

FÜHTBAUER, H. (1959) Die Schüttungen im Chatt und Aquitan der deutschen Apenvorlandmolasse. *Eclogae geol. Helv.*, 51, 928–941.

FÜCHTBAUER, H. (1964) Sedimentpetrographische Untersuchungen in der älteren Molasse nördlich der Alpen. *Eclogae geol. Helv.*, 57, 157–298.

GASSER, U. (1966) Sedimentologische Untersuchungen in der äusseren Zone der subalpinen Molasse des Entlebuchs (Kt. Luzern). *Eclogae geol. Helv.*, 59, 723–772.

GASSER, U. (1967) Erste Resultate über die Verteilung von Schwermineralen in verschiedenen Flyschkomplexen der Schweiz. *Geol. Rdsch.*, 56, 300–308.

GASSER, U. (1968) Die innere Zone der subalpinen Molasse des Entlebuchs (Kt. Luzern), Geologie und Sedimentologie. *Eclogae geol. Helv.*, 61, 229–313.

GIGER, M. & HURFORD, A.J. (1989) Tertiary intrusives of the Central Alps: their Tertiary uplift, erosion, redepostion and burial in the south-alpine foreland. *Eclogae geol. Helv.*, 82, 857–866.

GOHAIN, K. & PARKASH., B. (1990) Morphology of the Kosi Megafan. In: *Alluvial Fans: a Field Approach* (Ed. byA. H. Rachocki and M. Church), pp. 151–178. John Wiley, Chichester.

HELLER, P.L. & PAOLA, C. (1996) Downstram changes in alluvial architecture: an exploration of controls on channel stacking patterns. *J. sedim. Res.*, 66, 297–306, .

HOMEWOOD, P., ALLEN, P.A. & WILLIAMS, G.D. (1986) Dynamics of the Molasse Basin of western Switzerland. In: *Foreland Basins* (Ed. by P. A. Allen and P. Homewood), *Spec. Publ. Int. Ass. Sediment.*, 8, 199–217.

HUNZIKER, J.C., DESMONS, J. & HURFORD, A.J. (1992) Thirty-two years of geochronological work in the central and western Alps; a review of seven maps. *Mém. Geol. Lausanne*, 13.

HURFORD, A.J. (1986) Cooling and uplift patterns in the Lepontine Alps of South Central Switzerland and an age of vertical movement on the Insubric fault line. *Contr. Mineral. Petrol.*, 93, 413–427.

HURNI, A. (1991) *Geologie und Hydrogeologie des Truebtales.* Masters thesis, University of Bern.

JIN, J. (1995) Dynamic stratigraphic analysis and modelling in the southeastern German Molasse Basin. *Tübinger Geowissenschaftliche Arbeiten (TGA)*, A24.

JOHNSON, M.J., JORDAN, T.E., JOHNSSON, P.A. & NAESER, C.W. (1986) Magnetic polarity stratigraphy, age and tectonic setting of fluvial sediments in an eastern Andean foreland basin, San Juan Province, Argentina. In: *Foreland Basins* (Ed. by P. A. Allen and P. Homewood), *Spec. Publ. Int. Ass. Sediment.*, 8, 63–75.

JORDAN, T.E. (1981) Thrust loads and foreland basin evolution, Cretaceous, western United States. *Bull. Am. Ass. Petrol. Geol.*, 65, 2506–2520.

JORDAN, T.E., FLEMINGS, P.B. & BEER, J.A. (1988) Dating thrust-fault activity by use of foreland-basin strata. In: *New Perspectives in Basin Analysis* (Ed. by K. L. Kleinspehn and C. Paola), pp. 397–330. Springer-Verlag, New York.

KELLER, B. (1989) *Fazies und Stratigraphie der Oberen Meeresmolasse (Unteres Miozän) zwischen Napf und Bodensee.* PhD thesis, University of Bern.

KELLER, B. (1993) Hydrogeologie des schweizerischen Molasse-Beckens: Aktueller Wissensstand und weiterführende Betrachtungen. *Eclogae geol. Helv.*, 86, 573–652.

KLEIBER, K. (1937) Geologische Untersuchungen im Gebiet der Hohen Rone. *Eclogae geol. Helv.*, 30, 419–430.

LANG, S.C. & FIELDING, C.R. (1991) Facies architecture of a Devonian soft-sediment-deformed alluvial sequnence, Broken River Province, northeastern Australia. In: *The Three-Dimensional Facies Architecture of Terrigenous Clastic Sediments and its Implications for Hydrocarbon Discovery and Recovery* (Ed. by A. D. Miall and N. Tyler), *Spec. Publ. Soc. Econ. Paleont. Mineral., Concepts in Sedimentology and Paleontolgy*, 3, 122–132.

MATTER, A. (1964) Sedimentologische Untersuchungen im östlichen Napfgebiet (Entlebuch – Tal der Grossen Fontanne, Kt. Luzern). *Eclogae Geol. Helv.*, 57, 315–428.

MATTER, A., HOMEWOOD, P., CARON, C., RIGASSI, D., VAN STUJIVENBERG, J., WEIDMANN, M. & WINKLER, W. (1980) Flysch and Molasse of Western and Central Switzerland. In: *Geology of Switzerland, a Guidebook, (Part B Excursions)* (Ed. by R. Trümpy), pp. 261–293. Schweiz. geol. Komm.

MATTER, A., PETERS, T.J., BLÄSI, H.-R., MEYER, J., ISCHI, H. & MEYER, C.H. (1988a) Sondierbohrung Weiach, Geologie, Textband. *Geologische Berichte,* 6, Landeshydrologie und -geologie.

MATTER, A., PETERS, T., BLÄSI, H.-R., SCHENKER, F. & WEISS, H.-P (1988b) Sondierbohrung Schafisheim, Geologie, Beilagenband. *Geologische Berichte,* 8, Landeshydrologie und -geologie.

MAURER, H., GERBER, M.E. & NABHOLZ, W.K. (1982) Sedimentpetrographie und Lithostratigraphie der Molasse im Einzugsgebiet der Langete (Aarwangen – Napf, Oberaargau). *Eclogae geol. Helv.*, 75, 381–413.

MIALL, A.D. (1978) Lithofacies types and vertical profile models in braided river deposits: a summary. In: *Fluvial Sedimentology* (Ed. by A. D. Miall), *Mem. Can. Soc. Petrol. Geol.*, 5, 597–605.

MIALL, A.D. (1985) Architectural element analysis: a new method of facies analysis applied to fluvial deposits. *Earth-Sci. Rev.*, 22, 261–308.

MIALL, A.D. (1988) Reservoir heterogenities in fluvial sandstones: Lessons from outcrop studies. *Bull. Am. Ass. Petrol. Geol.*, 72, 682–697.

MIALL, A.D. (1991) Hierarchies of architectural units in terrigenous clastic rocks, and their relationship to sedimentation rate. In: *The Three-Dimensional Facies Architecture of Terrigenous Clastic Sediments and its Implications for Hydrocarbon Discovery and Recovery* (Ed. by A. D. Miall and N. Tyler), *Spec. Publ. Soc. Econ. Paleont. Mineral., Concepts in Sedimentology and Paleontolgy*, 3, 6–12.

MICHALSKI, I. & SOOM, M. (1990) The Alpine thermo-tectonic evolution of the Aar and Gotthard massifs, Central Switzerland: fission track ages on zircon and apatite and K-Ar mica ages. *Schweiz. Mineral. Petrogr. Mitt.*, 70, 373–387.

MILNES, A.G. & PFIFFNER, O.A. (1977) Structural development of the Infrahelvetic Complex, eastern Switzerland. *Eclogae geol. Helv.*, 70, 83–95.

MILNES, A.G. & PFIFFNER, O.A. (1980) Tectonic evolution of

the Central Alps in the cross section St. Gallen-Como. *Eclogae geol. Helv.*, 73, 619–633.

MITCHUM, R.M. (1977) Seismic stratigraphy and global changes of sea level, Part eleven: Glossary of terms used in seismic stratigraphy. In: *Seismic Stratigraphy – Application to Hydrocarbon Exploration* (Ed. by C. E. Payton), *Mem. Am. Ass. Petrol. Geol.*, 26, 205–212.

MITCHUM, R.M. & VAIL, P.R. (1977) Seismic stratigraphy and global changes of sea level, Part seven: seismic stratigraphy interpretation procedure. In: *Seismic Stratigraphy – Application to Hydrocarbon Exploration* (Ed. by C. E. Payton), *Mem. Am. Ass. Petrol. Geol.*, 26, 135–144.

MÜLLER, H.P. (1971) Geologische Untersuchungen in der subalpinen Molasse zwischen Einsiedeln und oberem Zürichsee (Kt. Schwyz). *Vjschr. natf. Ges. Zürich*, 16.

NADON, G.C. (1994) The genesis and recognition of anastomosed fluvial deposits: data from the St. Mary River Formation, southwestern Alberta, Canada. *J. sedim. Res.*, B64, 451–463.

PARKASH, B. & KUMAR, S. (1991) The Indo-Gangetic Basin. In: *Sedimentary Basins of India, Tectonic Context* (Ed. by S. K. Tandon, C. C. Pant and S. M. Casshypa), pp. 147–170. Gyanodaya Prakashan, Nainital, India.

PFIFFNER, O.A. (1986) Evolution of the north Alpine foreland basin in the Central Alps. In: *Foreland Basins* (Ed. by P. A. Allen and P. Homewood), *Spec. Publ. Int. Ass. Sediment.*, 8, 219–228.

PFIFFNER, O.A. (1992) Alpine orogeny. In: *The European Geotraverse* (Ed. by D. Blundell, R. Freeman S. and Müller), pp. 180–189. Cambridge University Press.

PFIFFNER, O.A., SAHLI, S. & STÄUBLE, M. (1996) Structure and evolution of the external basement massifs (Aar, Aiguilles Rouges/Mt. Blanc). In: *Deep Structure of the Swiss Alps: Results of the National Research Program 20 (NRP 20)* (Ed. by O. A. Pfiffner, P. Lehner, P. Heitzmann, St. Mueller and A. Steck), Schweiz. geol. Komm., in press.

PIERSON, T.C. & (1980), Erosion and deposition by debris flows at Mount Thomas, North Canterbury, New Zealand. *Earth Surf. Process.*, 5, 227–247.

PLATT, N.H. & KELLER, B. (1992) Distal alluvial deposits in a foreland basin setting – the Lower Freshwater Molasse (Lower Miocene), Switzerland: Sedimentology, architecture and palaeosols. *Sedimentology*, 39, 545–565.

PROSSER, S.D. (1993) Rift related depositional sequences and their seismic expression. In: *Tectonics and Seismic Stratigraphy* (Ed. by G. D. Williams and A. Dobb), *Spec. Publ. Geol. Soc. London*, 72, 35–66.

RAHN, M., MULLIS, J., ERDELBROCK, K. & FREY, M. (1994) Very low-grade metamorphism of the Taveyanne greywacke, Glarus Alps, Switzerland. *J. metam. Geol.*, 12, 625–641.

RAHN, M., MULLIS, J., ERDELBROCK, K. & FREY, M. (1995) Alpine Metamorphism in the North Helvetic Flysch of the Glarus Alps, Switzerland. *Eclogae geol. Helv.*, 88, 625–178.

RUST, B.R. (1978) Depositional models for braided alluvium. In: *Fluvial Sedimentology* (Ed. by A. D. Miall), *Mem. Can. Soc. Petrol. Geol.*, 5, 221–245.

SCHLANCKE, S. (1974) Geologie der subalpinen Molasse zwischen Biberbrugg/SZ, Hütten/ZH und Aegerisee/ZG, Schweiz. *Eclogae geol. Helv.*, 67, 243–331.

SCHLANKE, S., HAUBER, L. & BÜCHI, U. (1978) Lithostratigraphie und Sedimentpetrographie der Molasse in den Bohrungen Tschugg 1 und Ruppoldsried 1 (Berner Seeland). *Eclogae geol. Helv.*, 71, 409–425.

SCHLUNEGGER, F. (1995) *Magnetostratigraphie und fazielle Entwicklung der Unteren Süsswassermolasse zwischen Aare und Limmat*. PhD thesis, University of Bern.

SCHLUNEGGER, F., BURBANK, D.W., MATTER, A., ENGESSER, B. & MÖDDEN, C. (1996a) Magnetostratigraphic calibration of the Oligocene to Middle Miocene (30–15 Ma) mammal biozones and depositional sequences of the Swiss Molasse basin. *Eclogae geol. Helv.*, **89**, 753–788.

SCHLUNEGGER, F., MATTER, A., BURBANK, D.W. & KLAPER, E.M. (1996b) Magnetostratigraphic constraints on relationships between evolution of the central Swiss Molasse Basin and Alpine orogenic events. *Bull. Geol. Soc.* Am., in press.

SCHLUNEGGER, F., MATTER, A. & MANGE, M.A. (1993) Alluvial fan sedimentation and structure of the southern Molasse Basin margin, Lake Thun area, Switzerland. *Eclogae geol. Helv.*, 86, 717–750.

SCHMID, S.M., AEBLI, H.R., HELLER, F. & ZINGG, A. (1989) The role of the Periadriatic Line in the tectonic evolution of the Alps. In: *Alpine Tectonics* (Ed. by M Coward, D. Dietrich and R. G. Park), *Spec. Publ. Geol. Soc. London*, 45, 153–171.

SCHMID, S.M., FROITZHEIM, N., KISSLING, E., PFIFFNER, O.A. & SCHÖNBORN, G. (1996) Integrated geophysical-geological transect and tectonic evolution of the eastern Central Alps. In: *Deep Structure of the Swiss Alps: Results of the National Research Program 20 (NRP 20)* (Ed. by O. A. Pfiffner, P. Lehner, P. Heitzmann, St. Mueller and A. Steck), Schweiz. geol. Komm., in press.

SCHMID, S.M., ZINGG, A. & HANDY, M. (1987) The kinematics and movement along the Insubric line and the emplacement of the Ivrea Zone. *Tectonophysics*, 135, 47–66.

SCHÖNBORN, G. (1992) Alpine tectonics and kinematic models of the Central Southern Alps. *Mem. Sci. geol. Padova*, 44, 229–393.

SINCLAIR, H.P. & ALLEN, P.A. (1992) Vertical vs. horizontal motions in the Alpine orogenic wedge: stratigraphic response in the foreland basin.*Basin Res.*, 4, 215–232.

SINCLAIR, H.D., COAKLEY, B.J., ALLEN, P.A. & WATTS, A.B. (1991) Simulation of foreland basin stratigraphy using a diffusion model of mountain belt uplift and erosion: an example from the central Alps, Switzerland. *Tectonics*, 10, 599–620.

SINGH, H., PARKASH, B. & GOHAIN, K. (1993) Facies analysis of the Kosi megafan deposits. *Sediment. Geol.*, 85, 87–113.

SINHA, R. & FRIEND, P.F. (1994) River systems and their sediment flux, Indo-Gangetic plains, Northern Bihar, Inida. *Sedimentology*, 41, 825–845.

SOOM, M. (1990) Spaltspurdatierungen entlang des NFP 20-Westprofils (Externmassive und Penninikum). *Schweiz. Mineral. Petrogr. Mitt.*, 69, 191–192.

SPECK, J. (1953) *Geröllstudien in der subalpinen Molasse am Zugersee und Versuch einer paläogeographischen Auswertung*. PhD thesis, University of Zürich, Kalt-Zahnder, Zug.

STÜRM, B. (1973) *Die Rigischüttung. Sedimentpetrographie, Sedimentologie, Paläogeographie, Tektonik*. PhD thesis, University of Zürich.

VAKARCS, G., VAIL, P.R., TARI, G., PAGACSAS, G., MATTIC, R.E. & SZABO, A. (1994) Third order middle Miocene – early Pliocene depositional sequences in the prograding delta complex of the Pannonian Basin. *Tectonophysics*, 240, 81–106.

WERNER, D. (1980) Probleme der Geothermik im Bereich der Schweizer Zentralalpen. *Eclogae geol. Helv.*, 73, 513–525.

Manuscript received 6 December 1995; revision accepted 10 June 1996.